Lund university

MSFT01 - Master of Science Thesis

Impact of MLC shape smoothing on VMAT plan complexity and agreement between planned and delivered dose

Author:
Linnéa Strandell

Principal supervisor:
Anneli Edvardsson

Supervisors:
Hunor Benedek
Tobias Pommer &
Elinore Wieslander

Lund University

Abstract

Background/Purpose: The aperture shape controller (ASC) was introduced in the Eclipse treatment planning system to reduce plan complexity by counteracting irregular multileaf collimator (MLC) shapes. This should lead to decreased difference between the planned and measured dose distribution. The ASC was investigated to examine if it could limit plan complexity so that the planned and measured dose distributions are more consistent with each other, without compromising plan quality. The different ACS levels were studied with the aim to find the most optimal level regarding both agreement between measured and planned dose as well as plan quality.

Material and methods: Fifteen patients from three treatment sites; prostate, prostate including adjuvant lymph nodes (prostate lgl) and head and neck (H&N), were used in this study. A volumetric modulated arch therapy (VMAT) treatment plan using ASC level "Very low" was optimized for each patient. Six VMAT plans were then re-optimized for each of the patients using the same optimization objectives as for the original "Very low" plan, the only parameter changed was the ASC level. The plan quality was evaluated using homogeneity index (HI), conformity index (CI) and dose-volume histograms (DVH) parameters where the statistical significance was examined through Friedman tests and post hoc Wilcoxon tests. Two different complexity metrics, the modulated complexity score (MCS_v) and the edge area metric (EAM), were calculated for each treatment plan. The agreement between planned and delivered dose distribution was evaluated through measurements on a Varian TrueBeam using a Delta^4 phantom+ (ScandiDos AB). The correlation between the gamma analysis pass rate (3 % / 2 mm and 2 % / 2 mm) and plan complexity was analyzed using scatter plots and statistically investigated using Spearmans correlation tests.

Result: Generally, only small differences were observed in plan quality between the different ASC levels. In general, a higher ASC level decreased the complexity, and this trend was most prominent for the EAM. All plans passed the clinical pass rate at SUS (90 % for 3 % / 2 mm). A correlation between both investigated pass rates and EAM ($p = 0.000$ and $p = 0.000$) and MCS_v ($p = 0.003$ and $p = 0.045$) was detected for the prostate patients. No correlation was observed for the prostate lgl and H&N.

Conclusions: In general, the plan complexity decreased without compromising plan quality for higher ASC levels. However, a better agreement between the planned and delivered dose was not found. An ASC level between "Very low" and "High" is optimal as the plan quality is not affected and the plan complexity is reduced for these levels.

Popular scientific summary in Swedish:

En ny teknik som kan göra strålbehandlingsplaner mindre komplexa

Alla påverkas av cancer, direkt eller indirekt och under de senaste decennierna har antalet cancerfall ökat. Med strålbehandling kan man bekämpa cancern genom att bestråla tumören med joniserande strålning samtidigt som man försöker skydda omkringliggande frisk vävnad i den mån det går. Med dagens teknik kan man uppnå bättre tumörkontroll samtidigt som den friska vävnaden kan skyddas i större utsträckning, men i och med detta genereras även mer komplexa behandlingsplaner.

En vanlig strålbehandlingsteknik är "volumetric modulated arc therapy" (VMAT). Maskinen som används för att bestråla tumören roterar då runt patienten samtidigt som strålfältet formas (moduleras) med hjälp av bland annat en flerbladskollimator (MLC). MLCn består av flera små wolframblad vars öppning justeras under bestrålningen för att passa tumörens form samtidigt som hänsyn tas till riskorgan och tidigare dosbidrag med mera. Desto mer modulerad en plan är, desto mer komplex brukar den vara. VMAT-planer består ofta av små och oregelbundna MLC-öppningar, vilket innebär att det kan bli svårare att beräkna och leverera strålningen korrekt, man får alltså en än mer komplex plan. Detta kan i sin tur medföra en skillnad mellan den planerade och levererade strålningsfördelningen till patienten.

Ett försök till att lösa problemet med komplexa VMAT-planer är att göra MLC-formen jämnare. En ny funktion, som kallas "aperture shape controller" (ASC), har utvecklas av en leverantör för att göra just detta. Genom att använda ASCn förväntas skillnaden mellan den planerade och levererade strålningsfördelningen bli mindre.

ASCn har sex olika nivåer som avgör hur mycket vikt som läggs på att göra MLC öppningarna jämna. Syftet med detta arbete var att försöka identifiera en optimal ASC nivå genom att framställa VMAT-planer med olika ASC-nivåer för 15 patienter med prostatacancer och cancer i huvud/hals området. Planernas komplexitet och kvalité (d.v.s. hur väl planmålen uppfylls) beräknades och planerna levererades till ett mätfantom för att kunna jämföra skillnaden mellan den planerade och levererade strålningsfördelningen. Detta gjordes för att undersöka om ASCn kan begränsa komplexiteten utan att plankvalitén påverkas samt hitta en lämplig nivå på ASCn.

Resultatet från denna studie visar att ASCn jämnade ut MLC öppningen och gjorde den planerade behandlingsplanen mindre komplex utan att försämra plankvalitén i någon större utsträckning. Skillnaden mellan planerad och levererad stråldos tycks dock inte påverkas. Den optimala ASC nivån skiljer sig också mellan patienterna. Detta gör det svårt att bestämma vilken nivå som generellt är den bästa. Slutsatsen från dessa resultat är att använda näst högsta nivån eller lägre, dock inte ha den avstängd. Ytterligare studier med fler patienter behöver göras för att kunna precisera detta.

Acknowledgements

First, a thanks to my supporting supervisors:

Anneli Edvardsson for all your support and encouragement and for always being there to help me through this project with your knowledge.

Tobias Pommer for your enthusiasm and useful ideas and for sharing your expertise in plan complexity and explaining the MCS-code you provided.

Elinore Wieslander for your guidance with the plan quality metrics and your helpful advice.

Hunor Benedek for your insightful counsel and for your help with the phantom and statistics.

I would also like to thank:

Niklas Eliasson for learning me the system for treatment planning so that I could do my own simple VMAT plans and for planning the more difficult head and neck patients treatments.

Julia Götstedt at Sahlgrenska University Hospital for explaining and calculating the EAM for the treatment plans.

Jonas Scherman who developed the scripts used to evaluate the dosimetric parameters.

I'm very grateful for your help and support throughout this project, without each and every one of you I would not have gotten very far.

Abbreviations and acronyms

3DCRT - Three dimensional conformal radiation therapy
AAA - Anisotropic analytical algorithm
AAV - Aperture area variability
ASC - Aperture shape controller
CI - Conformity index
CT - Computed tomography
CTV - Clinical target volume
EBRT - External beam radiotherapy
GTV - Gross target volume
HI - Homogeneity index
H&N - Head and neck
HU - Hounsfield unit
IMRT - Intensity modulated radiotherapy
IMAT - Intensity modulated arc therapy
LINAC - Linear accelerator
LSV - Leaf sequence variability
MCS - Modulated complexity score
MLC - Multileaf collimator
MU - Monitor units
OAR - Organ at risk
PIV - Prescription isodose volume
PMMA - Polymethylmethacrylate
PO - Photon optimizer
PTV - Planning target volume
QA - Quality assurance
QC - Quality control
RT - Radiation therapy
SIB - Simultaneous integrated boost
SUS - Skånes universitetssjukhus (Skånes university hospital)
TV - Target volume
TPS - Treatment planning system
VMAT - Volumetric modulated arc therapy

Contents

1. Introduction

Since 1970, the number of cancer cases has more than doubled in Sweden and in 2018 more than 60 000 people were diagnosed with cancer [1, 2]. One way to treat cancer is through external beam radiotherapy (EBRT), where the aim is to kill cancer cells while trying to spare surrounding healthy tissue as much as possible [3].

In EBRT, ionizing radiation is generally produced by a linear accelerator (LINAC) where electrons are accelerated and hits a metal target. This impact will make the electrons slow down in a bremsstrahlung process creating high energy x-rays. The x-ray beam will pass through several different components in the LINAC gantry, one of them is the multileaf collimator (MLC). The MLC consists of a number of individual collimators (leaves), typically 5 or 10 mm wide, that move independently of one another to shape the beam after the tumor's size and shape while shielding organs at risk (OAR) for conventional EBRT [4].

Throughout the years different techniques have been developed in order to shape the beam more and more to the tumor and to spare OARs, i.e. making the dose distribution more conform to the treatment volume. The most common techniques used in a clinical environment today is three dimensional conformal radiation therapy (3DCRT) and volumetric modulated arc therapy (VMAT). The differences between the two methods is that forward planning is used for 3DCRT while VMAT uses inverse planning [5, 6, 7]. Forward planning means that the treatment consists of a number of static fields, set and shaped by the planner after the patient anatomy. For inversed planning the desired dose is described by goals and restrictions. The fields are then created and optimized through an automated iterative process that tries to solve the objectives for the desired dose distribution. For VMAT the gantry rotates around the patient in an arc, at the same time as the MLC moves, all under ongoing irradiation.

VMAT have led to better tumor control compared to 3DCRT [8, 9] at the expense of a low dose bath. VMAT technology has also reduced treatment time compared to intensity modulated radiation therapy (IMRT) [10]. However, VMAT treatment plans are in their nature more complex. This originates from the fact that treatments are delivered during continuous movement of gantry and MLC and dose rate modulation, as well as the iterative optimization process which tends to generate irregular MLC shapes and small leaf openings. This in turn makes it troublesome for the algorithms to calculate the dose accurately [11]. These plans may also be more difficult for the LINAC to deliver correctly, resulting in a difference between the planned and measured dose. At Skåne University Hospital (SUS), a dosimetric quality control (QC) measurement, of every VMAT plan is made before patient treatment to ensure that the difference between planned and measured dose is not too high.

To solve the problem with complex VMAT plans a new feature, called aperture shape controller (ASC), has been developed by Varian Medical Systems (Palo Alto, California, USA). The ASC will supposedly limit the plan complexity by making the MLC shape more even, i.e. small and irregular MLC shapes should be reduced [12]. The weight of the ASC differs between six levels from "Off" to "Very high". "Off" means it will not limit the MLC shape at all and "Very high" will limit the shape as much as possible. The ASC has not yet been fully tested and implemented in the clinic at SUS.

1.1 Aim

The aim of this thesis was to investigate if the ASC can limit the plan complexity so that the planned and measured dose distributions are more consistent with each other, without compromising plan quality. The different ACS levels were studied with the aim to find the most optimal level regarding both agreement between measured and planned dose as well as plan quality.

2. Background and theory

2.1 External beam radiotherapy

Before undergoing radiation therapy (RT), different imaging modalities can be used to locate the tumor. A computed tomography (CT) scan is performed on every patient in order to create a treatment plan. Multiple x-ray images are acquired during a CT by rotating the detector and x-ray source around the patient while moving the couch [13]. These images are reconstructed to get a set of images, each showing a slice of the patient's tissue structure. Each slice is built up by voxels, and each voxel value represents the attenuation of the photons. The attenuation measured in a voxel is related to the linear attenuation in water and air to get the Hounsfield Unit (HU), which is a standardized way to express CT numbers.

The images from the different modalities are used to define and delineate target volumes and OARs. The gross target volume (GTV) represents the volume where the tumor cell density is high [14]. The clinical target volume (CTV) includes the GTV and/or suspected tumor infiltration, i.e. microscopic malignant cells that may have spread outside the GTV. The planning target volume (PTV) includes the CTV and a margin where uncertainties in setup and internal movement are accounted for. OARs and other normal tissues, that might affect the treatment planning, are delineated as well.

Based on the delineated structures, a treatment plan is created using the CT images either through forward or inversed planning. The dose distribution is calculated with a dose calculation algorithm based on the translated HU values for each voxel in the CT image.

A quality assurance (QA) process can include several QC instances to verify that different steps in the workflow functions properly. To ensure the delivery system, i.e. the LINAC, performs as intended, a QC of the treatment plan is made, e.g. by delivering the treatment plan to a phantom. The measured dose distribution is then compared to the calculated/planned dose distribution. When the treatment plan is approved, regarding plan quality and delivery, the treatment of the patient can start.

2.2 Volumetric modulated arc therapy

IMRT was conceptually introduced by Brahme [5] in the late 80's. Compared to 3DCRT, inverse planning is applied. There are two IMRT methods, dynamic, where the MLC leaves move during irradiation and step-and-shoot, where the leaves only move when the beam is off [8]. With IMRT a better conformity was achieved, with improved target coverage while

sparing OAR to a greater extent. However, a larger volume of healthy tissue will receive low absorbed dose instead of a smaller proportion of healthy tissue receiving a higher dose ("low dose bath").

Yu [6] presented intensity modulated arc therapy (IMAT) in 1995. The gantry rotates around the patient in an arc, at the same time as the MLC moves, all under ongoing irradiation. However, several arcs (four to six arcs) were needed in order to deliver an adequate treatment plan as constraints on the MLC leaf position change had to be place in order for the gantry to move continuously, making the process time consuming.

Thirteen years later Otto [7] introduced VMAT to solve the problem with IMAT. One to two arcs could deliver the plan, making the process more time efficient. Today, VMAT is a commonly used technique to treat cancer patients. VMAT is more time efficient, accurate in delivery and a more conform method compared to 3DCRT and IMRT. For a VMAT treatment, the MLC shape, gantry rotation speed and dose rate varies continuously during irradiation.

A VMAT treatment plan is inversely optimized where the optimization parameters are MLC leaf position and monitor unit (MU) weights [7]. The optimization is done iteratively to find the minimum value of the objective function which governs the cost and goodness of the plan with a single value. The objective function is based on dose-volume constrains which are specified and prioritized by the operator to get the desired dose distribution.

For VMAT optimization in the Eclipse (Varian Medical Systems) treatment planning system (TPS), the optimization is divided into four so called multi-resolution (MR) levels [12]. In the first level, ten fixed angles over the arc, so called control points, are chosen for optimization and the objective function is calculated and driven towards its minimum. At the end of MR level 1, new control points are added in between the first ten and the optimization objectives are recalculated. This continues until MR level 4 when all control points (e.g. 178 control points for one arc) have been added.

2.3 Dose calculation

The absorbed dose distribution can be calculated with different algorithms. Generally the algorithms are divided into three groups according to how the transport of secondary particles is handled [15, 16]. For *type a* the lateral transport changes between different density regions are not modeled. The changes in lateral electron transport are approximately modeled for in *type b*. The further advanced type, *type c*, takes the change into consideration even more precisely. The HU values from the CT images are used to account for heterogeneities.

Eclipse has the option to use either *type b*; Anisotopic Analytical Algorithm (AAA) or *type c*; the Acuros XB, for photon beams to calculate the dose distribution for VMAT plans [12]. The AAA is a 3D pencil beam algorithm where the primary and secondary photons and scattered electrons are calculated from separated convolution models that are superpositioned. Scatter kernels, scaled in the lateral and longitudinal direction, are used to correct for heterogeneities. Acuros XB calculates the dose distribution even more accurately and the accuracy in the calculation is similar to Monte Carlo simulations. Acuros XB explicitly solves the equation that describes the linear macroscopic interactions of radiation particles; the linear Boltzmann transport equation.

2.4 Plan complexity

In this context, the term complexity refers to how complex the modulation is, i.e. how the photon fluence is altered. A treatment plan can be more or less modulated depending on patient anatomy, optimization constraints, TPS, TPS version, treatment design and LINAC abilities. The more modulated a plan is the more complex it becomes. To quantify the plan complexity different complexity metrics have been introduced. The metrics are often governed by LINAC parameters and plan properties like MU, fluence, gantry speed, dose rate and MLC positioning. Examples of such metrics are the modulated complexity score (MCS_v) [17] and the edge area metric (EAM) [18], which are described in more detail in section 2.4.2 and 2.4.3.

The different complexity metrics can complement or reduce time consuming QC measurements of treatment plans [19]. By scoring the complexity of a plan the choice between competing plans could be simplified. It could also be used to reduce the plan complexity at an early stage in the planning process. Finally, it has the potential to decide whether or not a QC measurement of a plan should be performed. The complexity of a treatment plan is, however, dependent on several various factors as stated above, and the different metrics takes different factors into consideration. Therefore, it may be necessary to use more than one metric.

When VMAT was introduced in the clinic it decreased treatment time leading to less patient motion and improved comfort for patients [20, 21]. However, due to inverse optimization VMAT plans may have small leaf gaps and irregular aperture shapes. The dose calculation for these irregular and small shaped segments can be less accurate compared to larger fields, due to lack of charged particle equilibrium [11]. With more complex apertures the demand on the leaf positioning accuracy also becomes greater making the dose delivery more difficult [22]. Hence, it would be desirable to find a way to reduce the plan complexity without compromising plan quality.

2.4.1 Aperture shape controller

The ASC can decrease the plan complexity by making the MLC shape more even [12]. This feature penalizes differences in adjacent MLC leaf positions to counteract irregular MLC shapes. The penalty is added to the objective function and the weight of it is chosen by the operator. There are six different levels; "Off", "Very low", "Low", "Moderate", "High" and "Very high". Figure 2.1 shows an example of the MLC shape for two different ASC levels for the same patient and gantry angle.

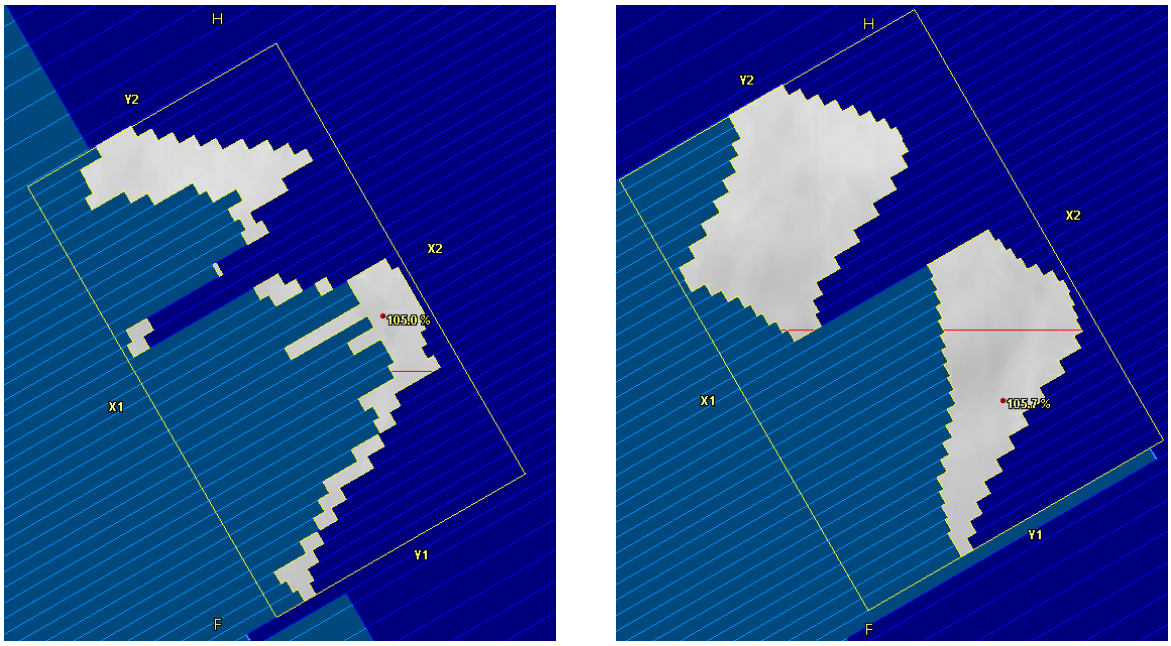

(a) **(b)**

Figure 2.1: Example of the MLC shape for ASC level "Very low" **(a)** and "Very high" **(b)**. The X1 MLC bank in light blue and the X2 bank in dark blue.

By controlling the aperture shape the plan complexity should be reduced leading to less QC failures and improved accuracy in dose delivery. For higher ASC levels the vendor recommends using convergence mode "on" or "extended" instead of "off", meaning that the number of iterations in the plan optimization is increased in the different MR levels. Convergence mode "on" increases the number of iterations compared to "off" by a factor of 2.5, 2.0, 1.0 and 1.0 for MR level 1, 2, 3 and 4 respectively.

2.4.2 Modulated complexity score

In 2010, McNiven et al. [17] combined MLC shape, aperture area and MU weight into a complexity metric for IMRT plans, the MCS. Irregular shape, small apertures and large MU differences leads to more complex plans. The score depends on the leaf sequence variability, aperture area variability and MU weight. Three years later, Masi et al. [23]

adjusted their definition to include VMAT plans, the MCS_v.

In the metric, the irregularity of the MLC shape is represented by the leaf sequence variability (LSV), which considers the position difference between the adjacent MLC leaves for both banks. The LSV for VMAT plans is defined as:

$$\mathrm{LSV}_{\mathrm{cp}} = \left(\frac{\sum_{n=1}^{N-1} (\mathrm{pos}_{\max} - |\mathrm{pos}_n - \mathrm{pos}_{n+1}|)}{(N-1) \cdot \mathrm{pos}_{\max}} \right)_{\mathrm{leftbank}} \cdot \left(\frac{\sum_{n=1}^{N-1} (\mathrm{pos}_{\max} - |\mathrm{pos}_n - \mathrm{pos}_{n+1}|)}{(N-1) \cdot \mathrm{pos}_{\max}} \right)_{\mathrm{rightbank}} \tag{2.1}$$

Leaves outside of the Y-jaws are not accounted for in this equation. N is the number of leaves and the leaf coordinate positions is denoted "pos". The change in position is relative to the maximum possible change in the control point according to:

$$\mathrm{pos}_{\max}(\mathrm{CP}) = \langle \max(\mathrm{pos}_{n \in N}) - \min(\mathrm{pos}_{n \in N}) \rangle \tag{2.2}$$

The variation in area is described by the aperture area variability (AAV). For each control point the distance between opposite leaves is calculated and normalized to the maximum area in the arc, which is defined by the maximum opening for each leaf pair over all control points in the arc. The AAV for VMAT is expressed as:

$$\mathrm{AAV}_{\mathrm{cp}} = \frac{\sum_{a=1}^{A} (\langle \mathrm{pos}_a \rangle_{\mathrm{leftbank}} - \langle \mathrm{pos}_a \rangle_{\mathrm{rightbank}})}{\sum_{a=1}^{A} (\langle \max(\mathrm{pos}_a) \rangle_{\mathrm{leftbank} \in \mathrm{arc}} - (\langle \max(\mathrm{pos}_a) \rangle_{\mathrm{rightbank} \in \mathrm{arc}}} \tag{2.3}$$

A is the number of leaves in the arc.

The MCS_v is calculated by weighting the mean value of $\mathrm{LSV}_{\mathrm{CP}}$ and $\mathrm{AAV}_{\mathrm{CP}}$ with the relative MU delivered between two consecutive control points, i.e. $\mathrm{CP}_{i,i+1}$, which is averaged over all the control points in the arc according to:

$$\mathrm{MCS}_v = \sum_{i=1}^{I-1} \left[\frac{(\mathrm{AAV}_{\mathrm{CP}i} + \mathrm{AAV}_{\mathrm{CP}i+1})}{2} \cdot \frac{(\mathrm{LSV}_{\mathrm{CP}i} + \mathrm{LSV}_{\mathrm{CP}i+1})}{2} \cdot \frac{\mathrm{MU}_{\mathrm{CP}i,i+1}}{\mathrm{MU}_{\mathrm{arc}}} \right] \tag{2.4}$$

The MCS_v varies between zero and unity, where a lower score signifies higher complexity.

2.4.3 Edge area metric

A different way to score the plan complexity is the EAM developed by Götstedt et al. [18]. It is based on the relative size of the region around the MLC edges defined accordingly:

$$\text{EAM} = \frac{R_1}{R_1 + R_2} \tag{2.5}$$

where R_1 and R_2 are different regions that the MLC openings are divided into. The area represented by the 5 mm distance on both sides of the MLC borders, 2.5 mm inside and outside of the opening, is confined as one region, R_1. The remainder of the open area within the MLC opening is accounted for in the other region, R_2. The result varies between zero and unity, where higher values of EAM represents a higher plan complexity, thus showing the opposite relationship as the MCS_v metric. Figure 2.2 shows an example of how R_1 is calculated, by taking 2.5 mm inside and outside the opening (white) for every leaf, for two different MLC openings represented by different ASC levels.

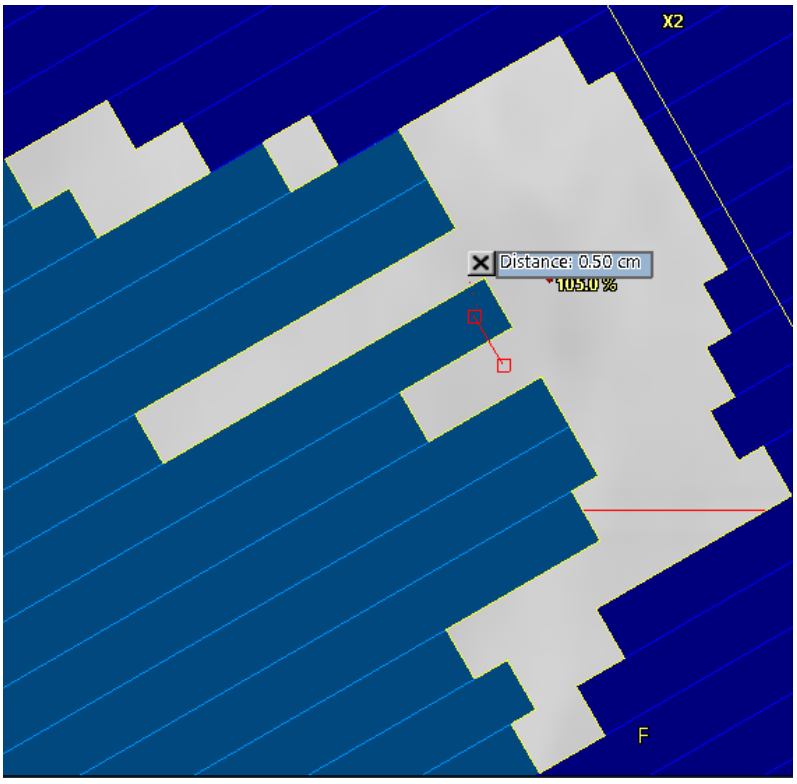

(a)

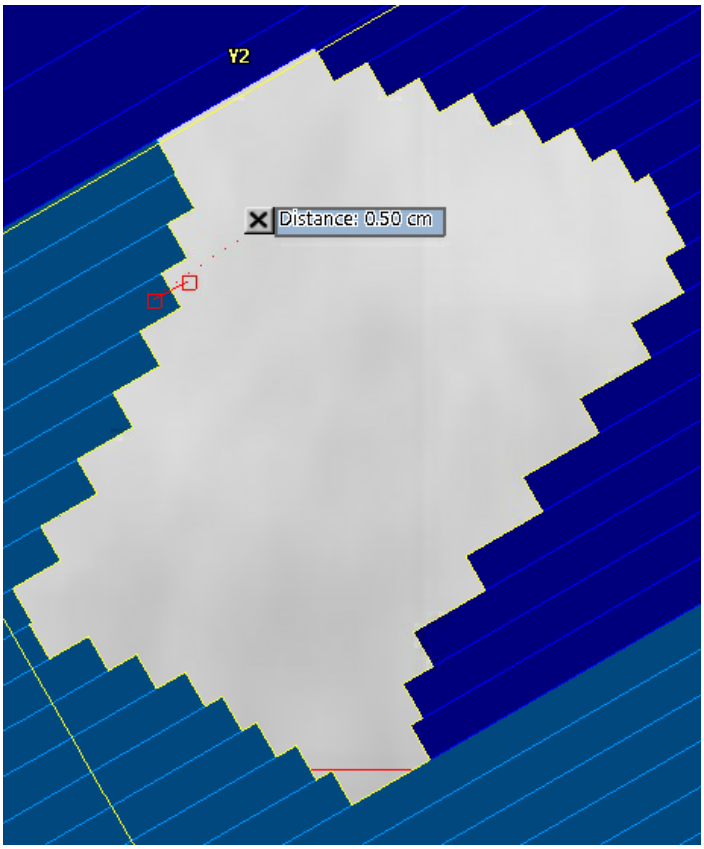

(b)

Figure 2.2: Example of how EAM is calculated for two different MLC openings with ASC level "Very low" **(a)** and "Very high" **(b)**. EAM will be much higher (and therefore more complex) for the MLC opening in **(a)** compared to **(b)** since the ratio of R_1 and R_2 will be much higher.

2.5 Delta^4 phantom

The dosimetric accuracy of a VMAT plan is often verified through a QC measurement before patient treatment, e.g. by delivering the planned treatment to a phantom and comparing the measured dose distribution with the calculated/planned dose distribution. An example of such a phantom is the wireless Delta^4 phantom+ (ScandiDos AB, Uppsala, Sweden). It is a Polymethylmethacrylate (PMMA) cylindrical phantom, with a diameter of 22 cm and length of 40 cm. It consists of two orthogonal detector planes containing 1069 p-Si diodes. The distance between the detector elements is 0.5 cm in the central area (6×6 cm^2) and 1 cm outside the centre [24]. The measured dose distribution is compared to the calculated dose distribution from the TPS through gamma evaluation, which is explained in section 2.6.4.

2.6 Evaluation

Different methods exist to evaluate plan quality, which in this context refers to the dosimetric parameters evaluated on the planned dose distribution, and for comparison of planned and measured dose distributions, the plan verification (QC). For example the plan quality can be analyzed with dose-volume histograms (DVH). Two other examples of plan quality metrics are the dose homogeneity and conformity [14]. To compare a planned and delivered dose distribution the so called gamma index may be used.

2.6.1 Dose-volume histogram

A DVH is calculated for the different delineated structures, and is often used to determine if the dose constraints in a clinical setting are fulfilled for the treatment plan and to compare different treatment plans. The voxels in the irradiated volume are sorted out with respect to the dose they have received for a given interval, and plotting the number of voxels as a function of the dose interval results in a differential DVH (figure 2.3 **(a)**) [4, 14]. Plotting the number of voxels that have received a minimum dose gives a cumulative DVH, i.e. a certain volume that receives a given dose or higher is plotted as a function of dose (figure 2.3 **(b)**). From the DVH different parameters, such as the minimum, maximum and mean dose as well as $D_{x\%}$ (dose received by $x\%$ of the volume) or $V_{x\text{Gy}}$ (volume that receives more than x Gy), can be retrieved. For example, $D_{2\%}$ is the near-maximum absorbed dose which is the highest absorbed dose that at least 2 % of the volume obtains.

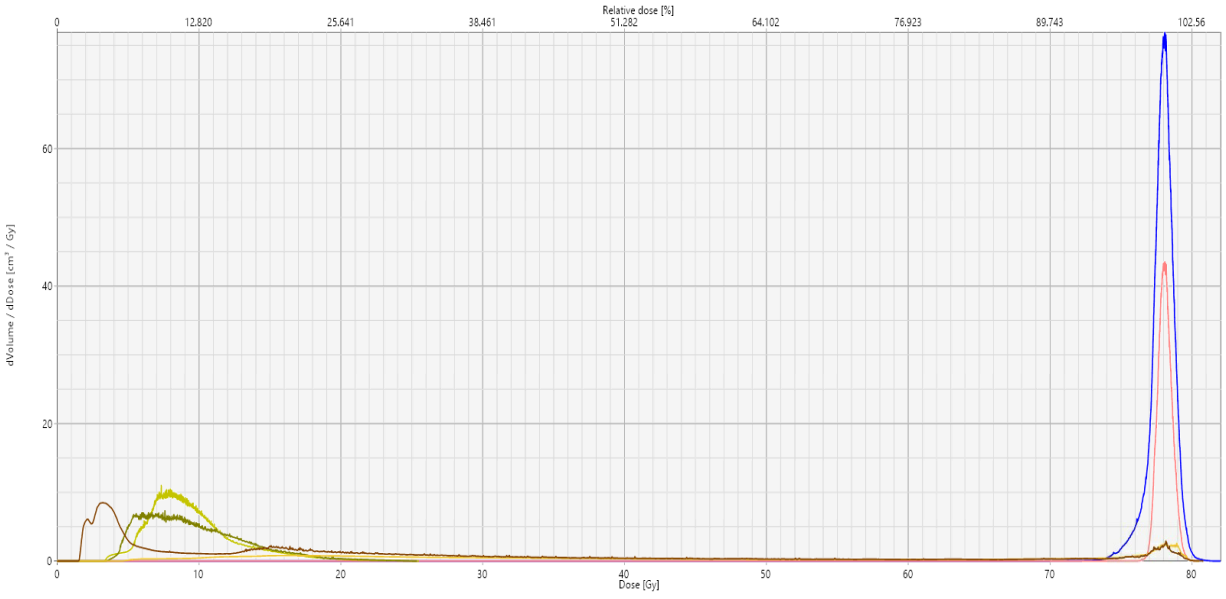

(a)

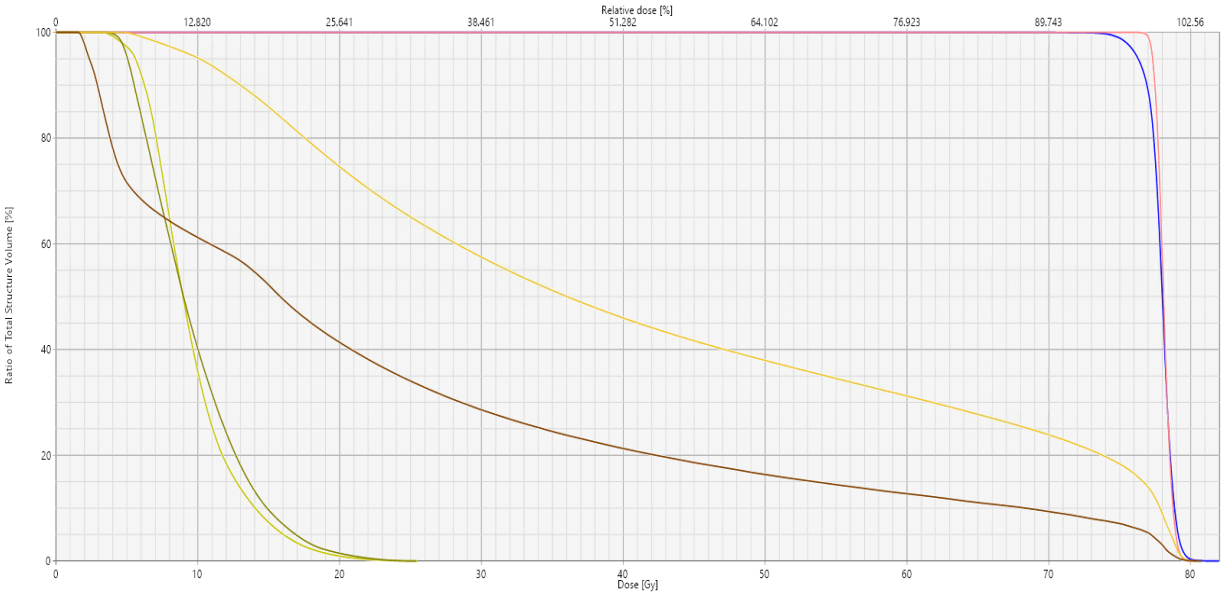

(b)

Figure 2.3: Example of **(a)** differential and **(b)** cumulative DVHs for the same prostate treatment plan, with the prescribed dose 78 Gy/39 fractions. The different lines represent the CTV (pink), PTV (blue), bladder (yellow), rectum (brown) and left and right femoral head (light and dark green, respectively).

2.6.2 Homogeneity index

The homogeneity index (HI) is a measure of how homogeneous the dose distribution is in the considered volume and there are a number of different definitions of it. ICRU - Report 83 [14] defines it as:

$$HI = \frac{(D_{2\%} - D_{98\%})}{D_{50\%}} \tag{2.6}$$

where $D_{2\%}$ is the near-maximum absorbed dose. The near-minimum absorbed dose, $D_{98\%}$, is the smallest absorbed dose covering 98 % of the volume. The index is normalized to $D_{50\%}$ which is the absorbed dose that 50 % of the volume receives. A low HI value represents high homogeneity.

2.6.3 Conformity index

The conformity index (CI) is a measure of the overlap between a certain isodose volume and the volume of the PTV [14, 25]. A good fit around the tumor is indicated by $CI = 1$ and $CI = 0$ represents a poor fit. There are different ways to calculate the CI. In the method suggested by Paddick [25] CI is calculated as:

$$CI = \frac{TV_{PIV}}{TV} \cdot \frac{TV_{PIV}}{PIV} = \frac{TV_{PIV}^2}{(TV \cdot PIV)} \tag{2.7}$$

where PIV stands for prescription isodose volume and TV for target volume. Hence, TV_{PIV} is the target volume covered by the prescription isodose volume. This method equally accounts for under- and overdosage.

2.6.4 Gamma index

Low et al. [26] introduced gamma evaluation as a method to compare planned and measured dose distributions. It combines two existing methods, the distance to agreement (DTA) and dose difference, into a numerical index, the gamma index.

Dose difference, or dose deviation, is the difference between calculated, D_c, and measured, D_m, dose, for every position, $\boldsymbol{r}$. To determine the DTA, the distance between a point in the measured data, $\boldsymbol{r}_m$, and the closest point in the calculated data, $\boldsymbol{r}_c$, with the same dose is calculated. The dose deviation is more suitable for volumes with a low dose gradient whilst the DTA is more suitable in regions with a high dose gradient. The gamma evaluation concept combines these two methods into one metric where DTA and dose difference are assumed to be equally important.

For each measured point, a gamma value is computed according to:

$$\Gamma = \sqrt{\frac{r^2(\boldsymbol{r}_m, \boldsymbol{r}_c)}{\Delta d_M^2} + \frac{\delta^2(\boldsymbol{r}_m, \boldsymbol{r}_c)}{\Delta D_M^2}} \tag{2.8}$$

where ΔD_M is the dose difference criterion and Δd_M is the criterion for the DTA. The expression for the dose difference, $r(\boldsymbol{r}_m, \boldsymbol{r}_c)$, and DTA, $\delta(\boldsymbol{r}_m, \boldsymbol{r}_c)$, are determined by:

$$r(\boldsymbol{r}_m, \boldsymbol{r}_c) = |\boldsymbol{r}_c - \boldsymbol{r}_m| \tag{2.9}$$

and

$$\delta(\boldsymbol{r}_m, \boldsymbol{r}_c) = D_c(\boldsymbol{r}_c) - D_m(\boldsymbol{r}_m) \tag{2.10}$$

The minimum gamma value defines the gamma index according to:

$$\gamma(\boldsymbol{r}_m) = \min\left\{\Gamma\left(\boldsymbol{r}_m, \boldsymbol{r}_c\right)\right\} \forall \left\{\boldsymbol{r}_c\right\} \tag{2.11}$$

A point passes the evaluation if $\gamma(\boldsymbol{r}_m) \leq 1$ and fails if $\gamma(\boldsymbol{r}_m) > 1$. The gamma pass rate is the fraction of the examined points that passes the gamma criteria.

3. Material and method

3.1 Patient data

In this study, 15 patients previously treated with EBRT at SUS were included. Ten prostate cancer cases and five oropharynx cancer cases. The CTV included only the prostate for five cases (P1-P5) and for the other five the prostate as well as adjuvant lymph nodes (prostate lgl) in the pelvis were included (P6-P10). The CTV for the head and neck (H&N) cases (P11-P15) included one or both tonsils and adjuvant lymph nodes. The original delineation of the GTV, CTV, PTV and OARs from the clinical treatment plans were kept for all patients The prescribed absorbed dose was 2 Gy per fraction, resulting in a total dose of 78 Gy, 50 Gy and 68/54.4 Gy for the prostate, prostate lgl and H&N patients, respectively. The H&N patients were planned with a Simultaneous Integrated Boost (SIB) with two dose levels, 68 Gy to the primary tumor and 54.4 Gy to adjuvant lymph nodes. Figure 3.1 shows examples of delineated structures for the three patient cohorts.

(a) **(b)** **(c)**

Figure 3.1: An example of the delineation for a prostate patient **(a)**, prostate lgl patient **(b)** and a H&N patient **(c)**. The CTV and PTV are represented by the pink and blue lines respectively. For **(a)** and **(b)** OARS shown in the figure are rectum (brown), bladder (yellow) and left (light green) and right (dark green) femoral head. In **(b)** the bowelbag is represented by the orange line. Panel **(c)** shows left (light purple) and right (dark purple) parotis, spinal cord (yellow), mandible (grey) and the oral cavity (brown-green).

3.2 Treatment planning and optimization

Initially, one plan was optimized for each patient using the Eclipse TPS photon optimizer (PO) version 15.6.05, with the ASC level set to "Very low" as this level was believed to result in a relatively complex plan as a starting point for the other ASC levels. Convergence mode "on" was used and jaw tracking was activated. Plans were optimized for a TrueBeam LINAC equipped with the Millennium 120 leaf MLC (Varian Medical Systems),

where the leaf width for the 40 central leaf pairs was 5 mm, and for the ten outer leaf pairs, 10 mm. The collimator angle was set to 30° and the energy 6 MV with flattening filter was used. No MU restrictions were used. To get a complex plan the absorbed dose to the OARs were restricted as much as possible, while still trying to maintain the CTV and PTV coverage according to planning constraints at SUS. A selection of the clinical criteria at SUS where evaluated. These DVH parameters are specified in tables 3.1 - 3.3. The absorbed dose distribution was calculated with the AAA using a grid of 2.5 mm as this is used in the clinic. For each patient, the treatment plan was duplicated six times and only the ASC level was changed between the plans. The same optimization objectives were used to isolate the effect of the ASC. Plans for all ASC levels, including the initial plan with ASC "Very low", and the ASC turned "Off" were created. The plans were re-optimized from the start and both the automatic optimization mode and automatic intermediate dose (starting from MR level 3) were used. In total, 90 VMAT plans were generated.

Table 3.1: Selection of dose constraints for treatment planning of only prostate cancer with 78 Gy/39 fractions at SUS Lund.

Priority	Structure	Dose/Volume recommendations
1	CTV Prostate	$D_{\text{min}} \geq 76$ Gy
2	PTV prostate	$D_{95\%} \geq 75$ Gy
3	Rectum	$V_{70\text{Gy}} < 15$ %
4	PTV prostate	$D_{98\%} \geq 74$ Gy
5	Rectum	$V_{75\text{Gy}} < 10$ %
6	Capiti femorales	$D_{2\%} \leq 55$ Gy
7	Rectum	$V_{60\text{Gy}} < 30$ %
8	Body	$D_{\text{max}} \leq 82$ Gy
9	Bladder	$D_{\text{ave}} \leq 62$ Gy

Table 3.2: Selection of dose constraints for treatment planning of prostate lgl with 50 Gy/25 fractions at SUS Lund.

Priority	Structure	Dose/Volume recommendations
1	CTV Prostate	$D_{\text{min}} \geq 47.4$ Gy
2	Rectum	$V_{45\text{Gy}} < 20$ %
3	Rectum	$V_{48\text{Gy}} < 15$ %
4	PTV lymph nodes	$D_{99\%} \geq 46.5$ Gy
5	Capiti femorales	$D_{\text{max}} \leq 35.3$ Gy
6	Bowelbag*	$V_{30\text{Gy}} < 300$ cm^3
		$V_{40\text{Gy}} < 150$ cm^3
		$V_{45\text{Gy}} < 100$ cm^3
		$V_{50\text{Gy}} < 35$ cm^3
7	Rectum	$V_{38\text{Gy}} < 35$ %
8	Body	$D_{\text{max}} \leq 52.6$ Gy
9	Bladder	$D_{\text{ave}} \leq 39.7$ Gy

*The PTV volume is excluded with a margin of 5 mm.

Table 3.3: Selection of dose constraints for treatment planning of H&N, 68 and 54.4 Gy/34 fractions at SUS Lund.

Priority	Structure	Dose/Volume recommendations
1	Spinal cord	$D_{\text{max}} \leq 48$ Gy
2	PTV (all)	$D_{98\%} \geq 95$ %
3	Parotid	$D_{\text{ave}} \leq 20$ Gy
4	Larynx	$D_{\text{ave}} \leq 40$ Gy
5	Oral cavity	$D_{\text{ave}} \leq 24$ Gy
6	Submandibularis	$D_{\text{ave}} \leq 39$ Gy
7	Mandible	$D_{2\%} \leq 68$ Gy

3.3 Treatment plan measurements

Verification plans were created in Eclipse by transferring the treatment plan to the Delta^4 phantom+. The treatment plan, based on the CT images of the patient, was recalculated to a verification plan based on the shape and HU values of the Delta^4 phantom+. A Varian TrueBeam LINAC was used to deliver the treatment plans to the Delta^4 phantom+.

The phantom was positioned on the treatment couch (figure 3.2) using the LINAC field crosshair. Following the clinical routine at SUS, a static 10×10 cm^2 reference field, with gantry angle 45°, was first delivered to correct for the output variation of the machine. To make sure that the phantom had been correctly set up in the LINAC's isocenter, the "optimize phantom position" tool was used for every patient's base plan (ASC level "Very low"), in order to be consistent. If the vertical, longitudinal and/or lateral position was off by more than 0.2 cm, the phantom position was adjusted by moving the couch as the software suggested. The phantom position was then verified by delivering the routine static reference field and using the "optimize phantom position" tool. The treatment plans were then delivered and measured. The Delta^4 measurement results presented in this thesis were performed on four different occasions, but all six plans for a patient were always measured on the same occasion.

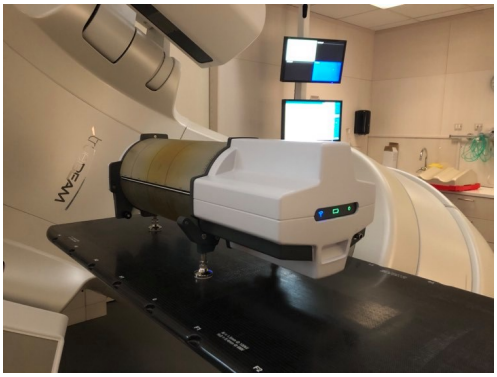

Figure 3.2: Setup of the Delta^4 phantom+.

3.4 Evaluation and comparison

The dosimetric parameters in tables 3.1-3.3 together with the CI (equation (2.7)) and HI (equation (2.6)) values for the PTV were used to analyze the plan quality. These parameters were computed using in-house developed scripts in Eclipse. For the H&N patients, both tonsils were included in the CTV for two of them (P14 and P15). For these patients the side which received the lowest dose was considered as the contralateral side.

To evaluate the plan complexity, EAM and MCS$_v$ were calculated for each plan according to equation (2.4) and (2.5). An in-house developed MatLab (The MathWorks Inc.) code was used to calculate the MCS$_v$. The EAM was calculated using MatLab at Sahlgrenska University Hospital [18]. Both calculations were based on the DICOM RP files.

The measurements were evaluated using gamma evaluation in the Delta^4 software according to equations (2.8-2.11). The criteria for the gamma analysis at SUS is $\Delta D_M = 3$ % and

$\Delta d_M = 2$ mm (3 % / 2 mm) with a pass rate of 90 %. In this study two different criteria for the gamma analysis, 3 % / 2 mm and 2 % / 2 mm (global dose and cut-off dose of 15 %), were used. The 3 % / 2 mm is used at SUS for clinical evaluation and the 2 % / 2 mm was evaluated to investigate if bigger differences could be observed for stricter criteria.

3.5 Statistical analysis

IBM SPSS Statistics version 26 was used for all statistical analysis. A Shapiro-Wilk normality test was carried out for the variables to check if they where normally distributed, with a significance level of 0.05. Since the sample sizes were small and the Shapiro-Wilk tests showed that not all data was normally distributed, non-parametric tests were carried out.

Friedman's test is a non-parametric test that consider repeated measures, and is used to test the difference between more than two groups. This test was used to examine if there were any statistically significant differences in the dosimetric parameters for the different ASC levels. If a statistically significant difference was found, post hoc Wilcoxon's tests were performed. This is a non-parametric test which is used for two groups. A significance level of 0.05 was used, not Bonferroni adjusted as the number of comparisons were so large it was considered to be too conservative.

To investigate the correlation between the pass rate and complexity metrics Spearman's correlation coefficients, r_S, were calculated and a significance level of 0.05 was used. This non-parametric test checks if a monotonic correlation between two variables exist and what the strength and direction of this relationship is. A r_S value of 0.8 or over is considered a strong correlation while a value between 0.5-0.8 is considered as a moderate correlation. Values between 0.3 and 0.5 are regarded as weak correlations and values below 0.3 indicates no correlation.

4. Results

4.1 Plan quality

The relative differences in the dosimetric parameters between each ASC level and the ASC level "Very low" are presented in figures 4.1-4.3 for the three different patient cohorts; prostate, prostate lgl and H&N. For the bowelbag, the absolute differences are presented.

The results of the statistical tests for the dosimetric parameters showing a statistically significant difference are summarized in table A.1 in Appendix A. In general, only small differences were observed in plan quality between the different ASC levels. For the H&N patients, no significant differences were found in the dosimetric parameters. However, a higher ASC level resulted in improved conformity. For prostate and prostate lgl a statistically significant difference was found for some of the dosimetric parameters. In most cases the difference was observed between "Very high" and the lower three ASC levels. The CTV coverage was improved for both prostate cohorts and the rectum dose was decreased for the higher ASC levels ("High" and "Very high") for prostate + lgl patients. However, the PTV coverage, CI and HI was worse and the other OAR doses increased for "Very high", except for $V_{50\text{Gy}}$ for bowelbag where a statistical significance was found using the Friedman's test, however, not with the Wilcoxon's test.

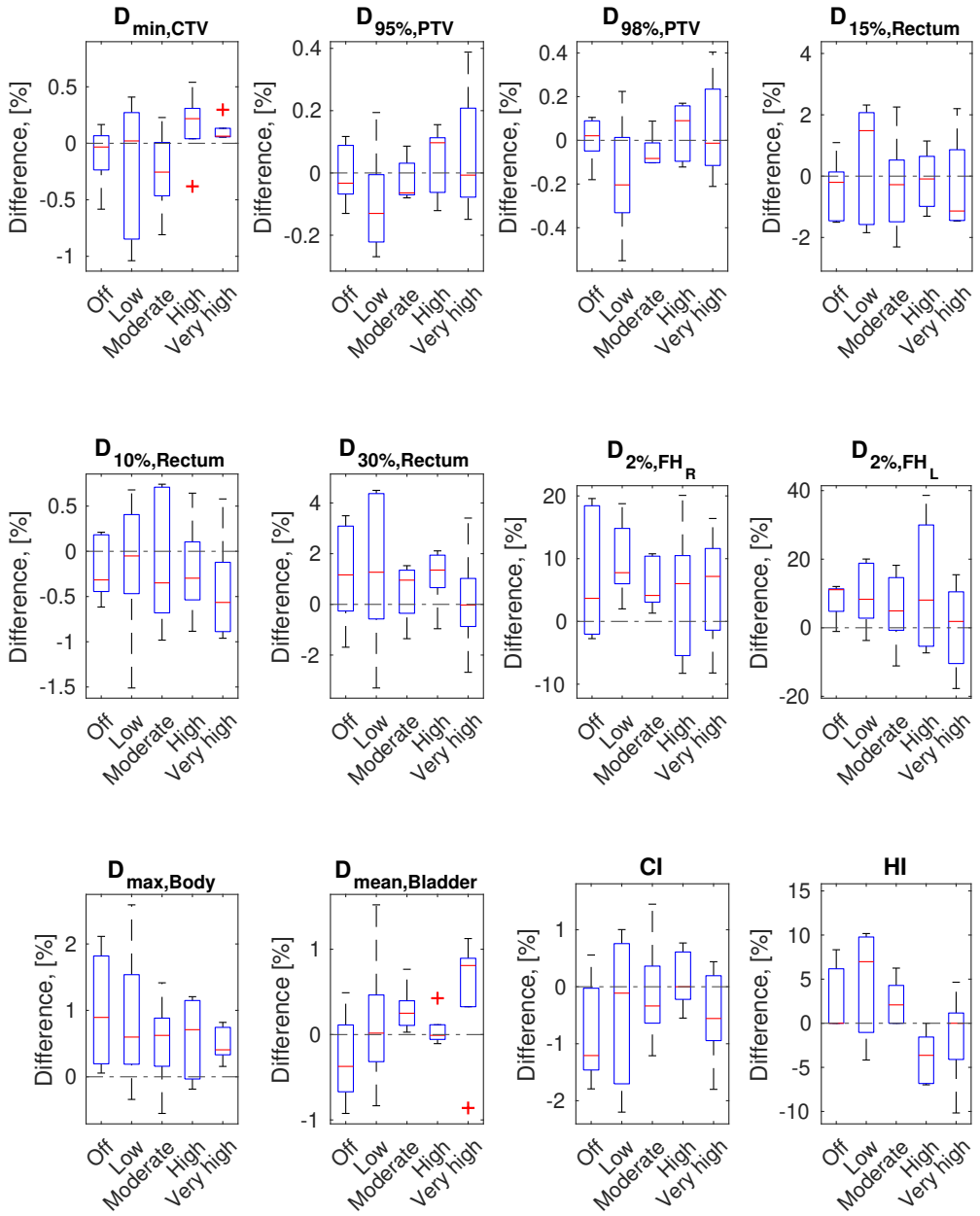

FH: Femoral head; L: Left; R: Right

Figure 4.1: Relative differences in dosimetric parameters for the ASC levels relative to ASC "Very low" for the prostate only cases. The dashed-dotted line at zero represents the "Very low" setting. The blue box represents the 25th and 75th percentile, the red line within the boxes signifies the median and the range is specified by the dashed line. Outliers are represented by a red plus sign.

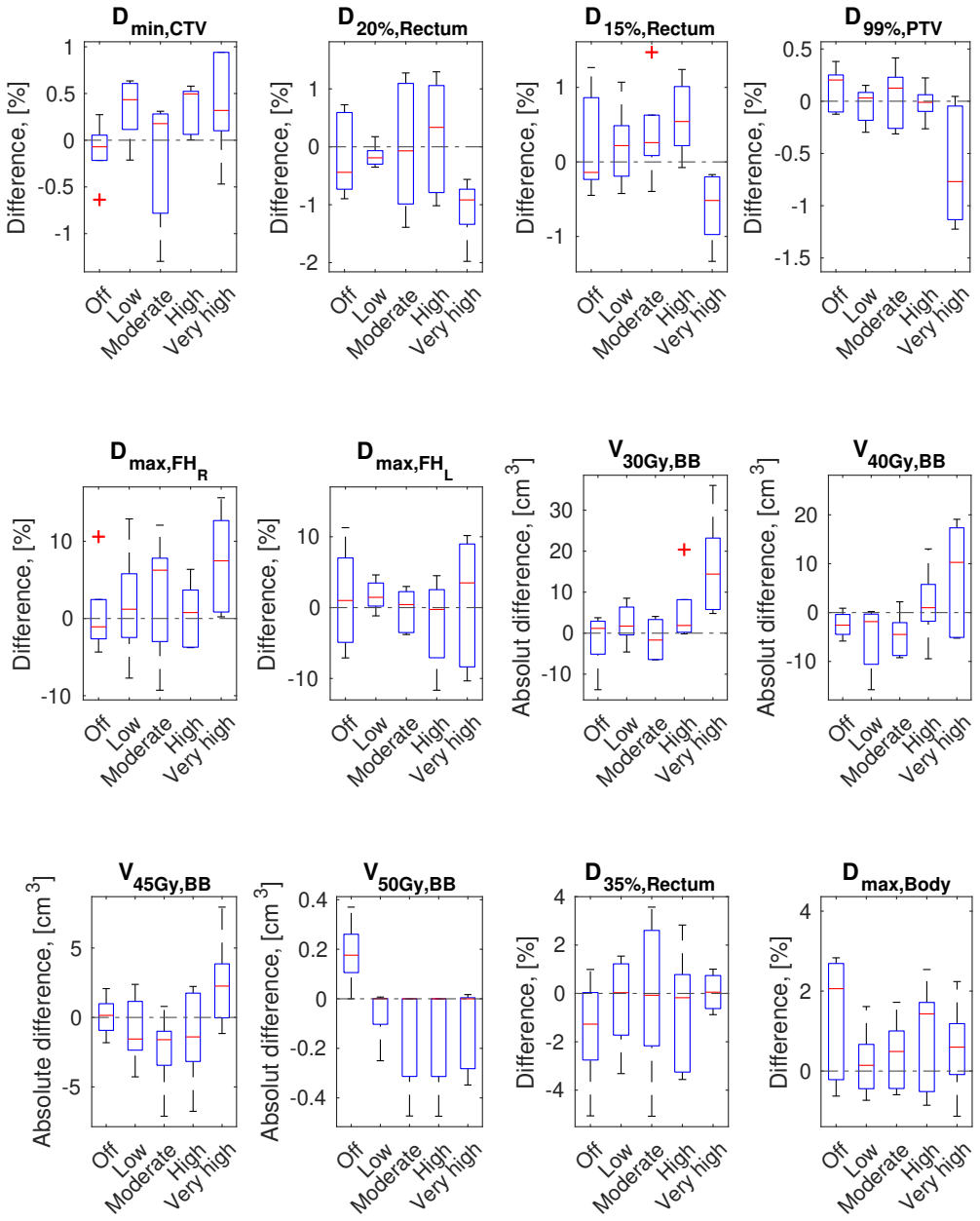

BB: Bowelbag; FH: Femoral head; L: Left; R: Right

Figure 4.2: Relative differences in dosimetric parameters for the ASC levels relative to ASC "Very low" for the prostate lgl cases. Relative differences are presented for all structures except the bowelbag where the absolute differences are presented.

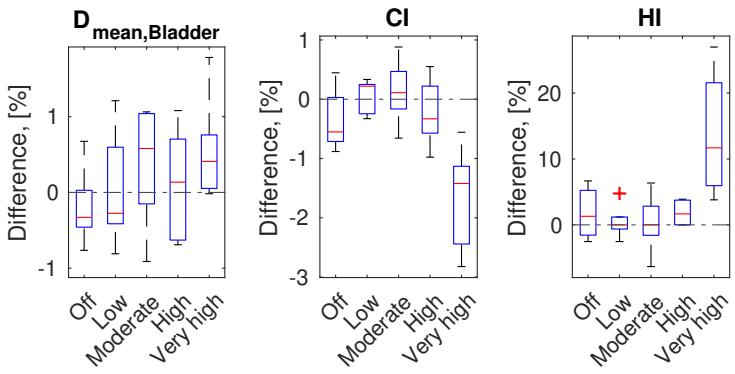

Figure 4.2: Continued.

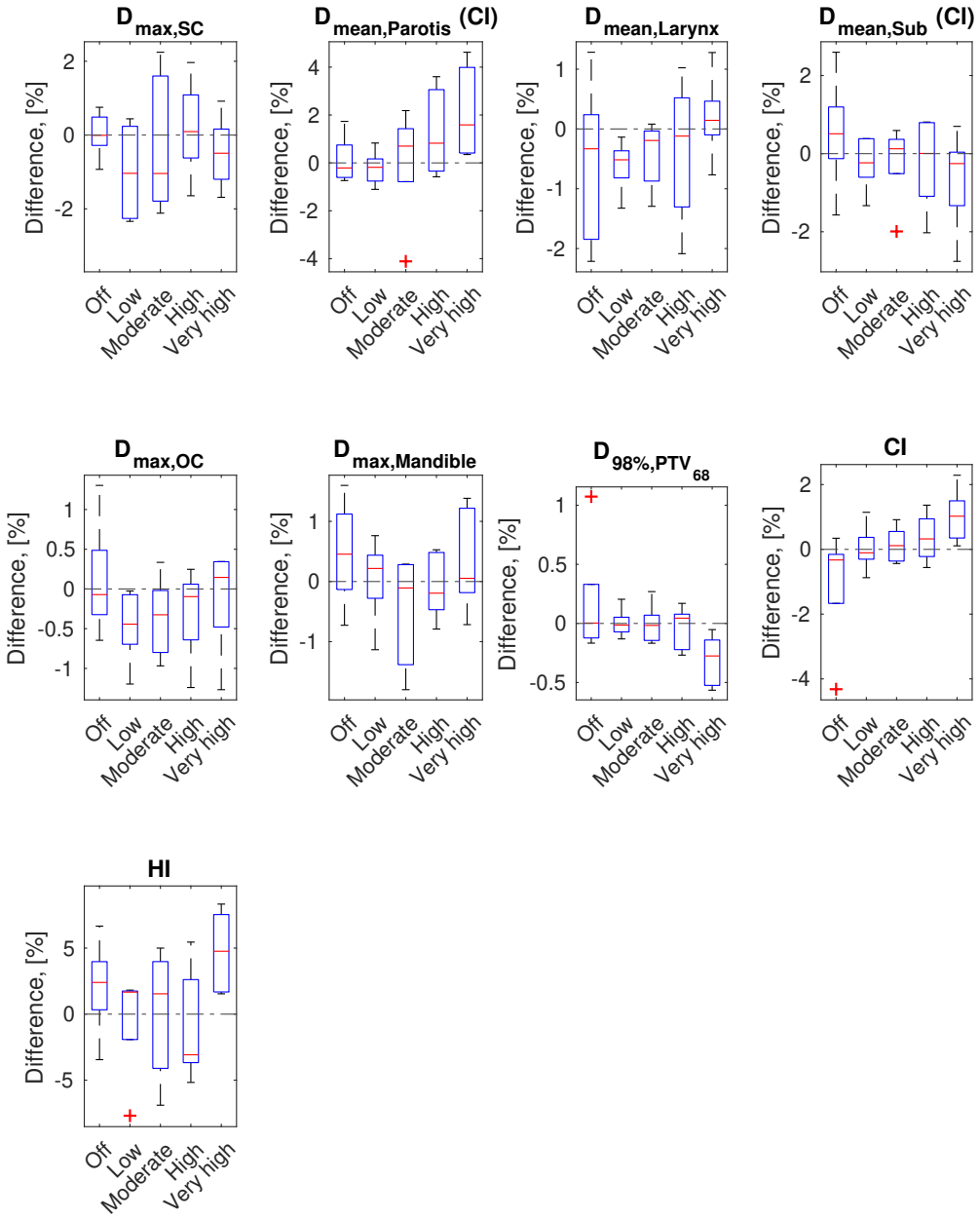

Cl: Contralateral side; OC: Oral cavity; SC: Spinal cord; Sub: Submandibularis;.

Figure 4.3: Relative differences for the dosimetric parameters for the ASC levels relative to ASC "Very low" for the H&N cases.

4.2 Complexity metrics

To evaluate the complexity of the treatment plans, two complexity metrics were calculated, the EAM and MCS_v (equation (2.4) and (2.5)). A high MCS_v value indicates a less complex plan while the EAM indicates the opposite, a low EAM means a less complex plan. The mean MCS_v and EAM for each plan as a function of ASC level are shown in figure 4.4. As expected, the complexity appears to decrease for higher ASC levels, especially for the prostate lgl and H&N patients. A more distinct trend is observed for the EAM than for the MCS_v. The level being most complex varied between the patients, for example ASC setting "Very low" is less complex than "Low" for P5. This variation is more distinct for the MCS_v.

Figure 4.5 and 4.6 presents the mean LSV and AAV as a function of ASC level for each plan. The LSV appears to increase for an increasing ASC level. This seems to be the case for the AAV as well, although the tendency is weaker as the AAV varies more between the different levels. No obvious trend was observed for the total number of MUs for the prostate and prostate lgl patients, whereas a slight decrease with increasing ASC level might be visible for the H&N cohort (figure 4.7).

For two of the patients (P7 and P9) two new base plans were generated, one with lower complexity and one with higher. This was done to examine how the ASC was affected by the initial plan complexity. The complexity score as a function of ASC levels showed the same tendency as the whole cohort.

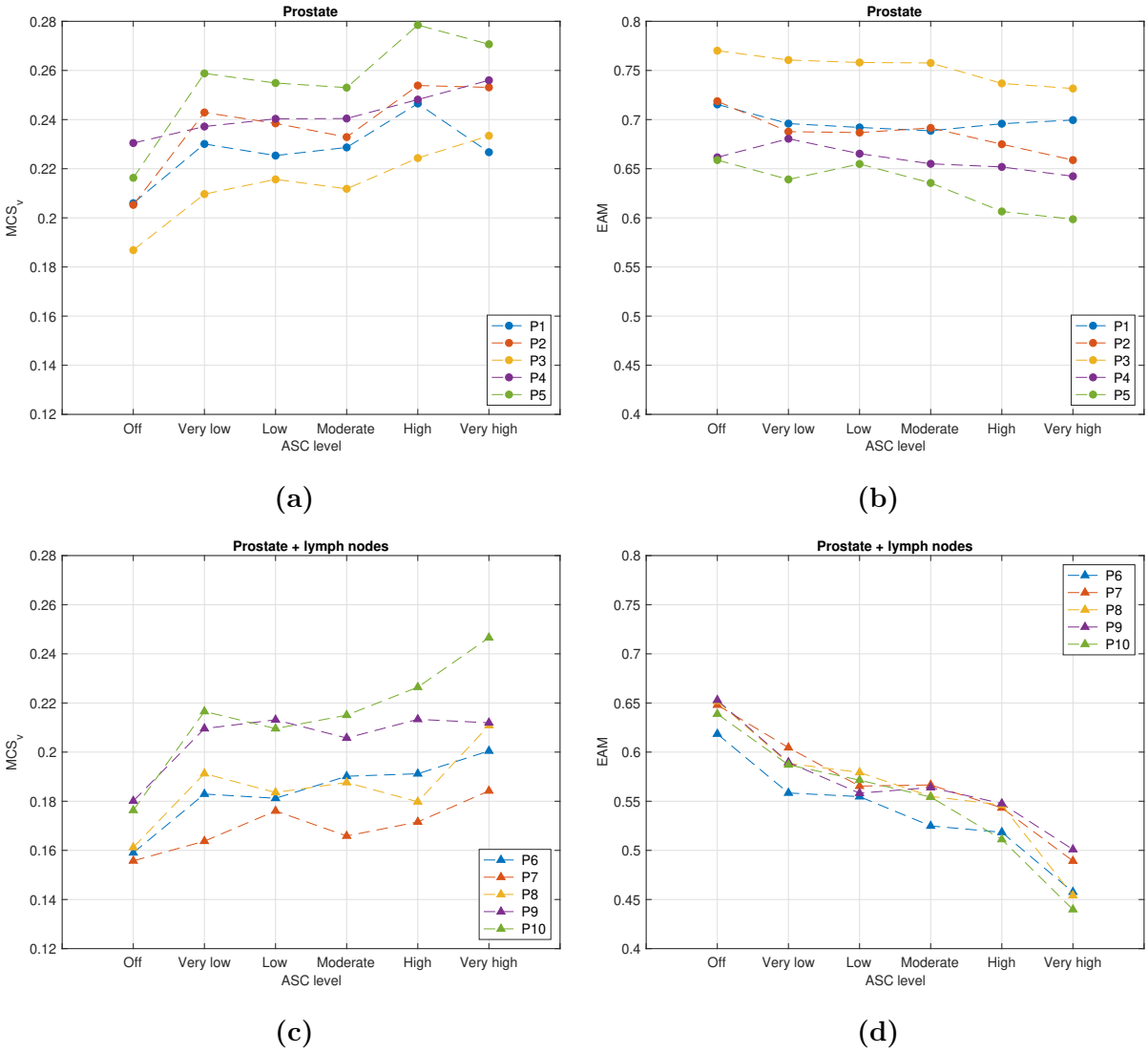

Figure 4.4: The MCS$_v$ (left panel) and EAM (right panel) as a function of ASC level for the different groups; prostate **(a)** and **(b)**, prostate lgl **(c)** and **(d)**, H&N **(e)** and **(f)**.

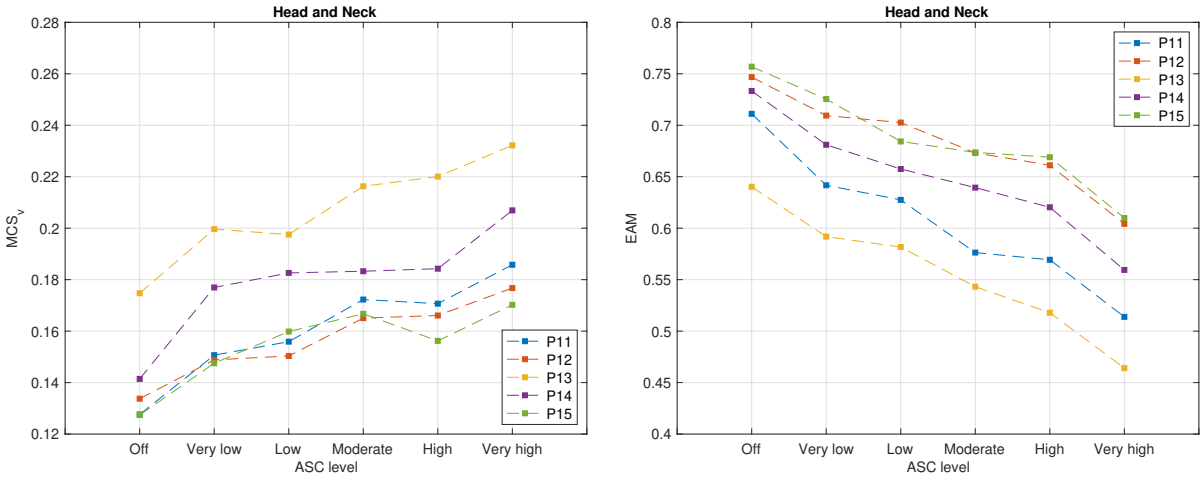

(e) **(f)**

Figure 4.4: Continued.

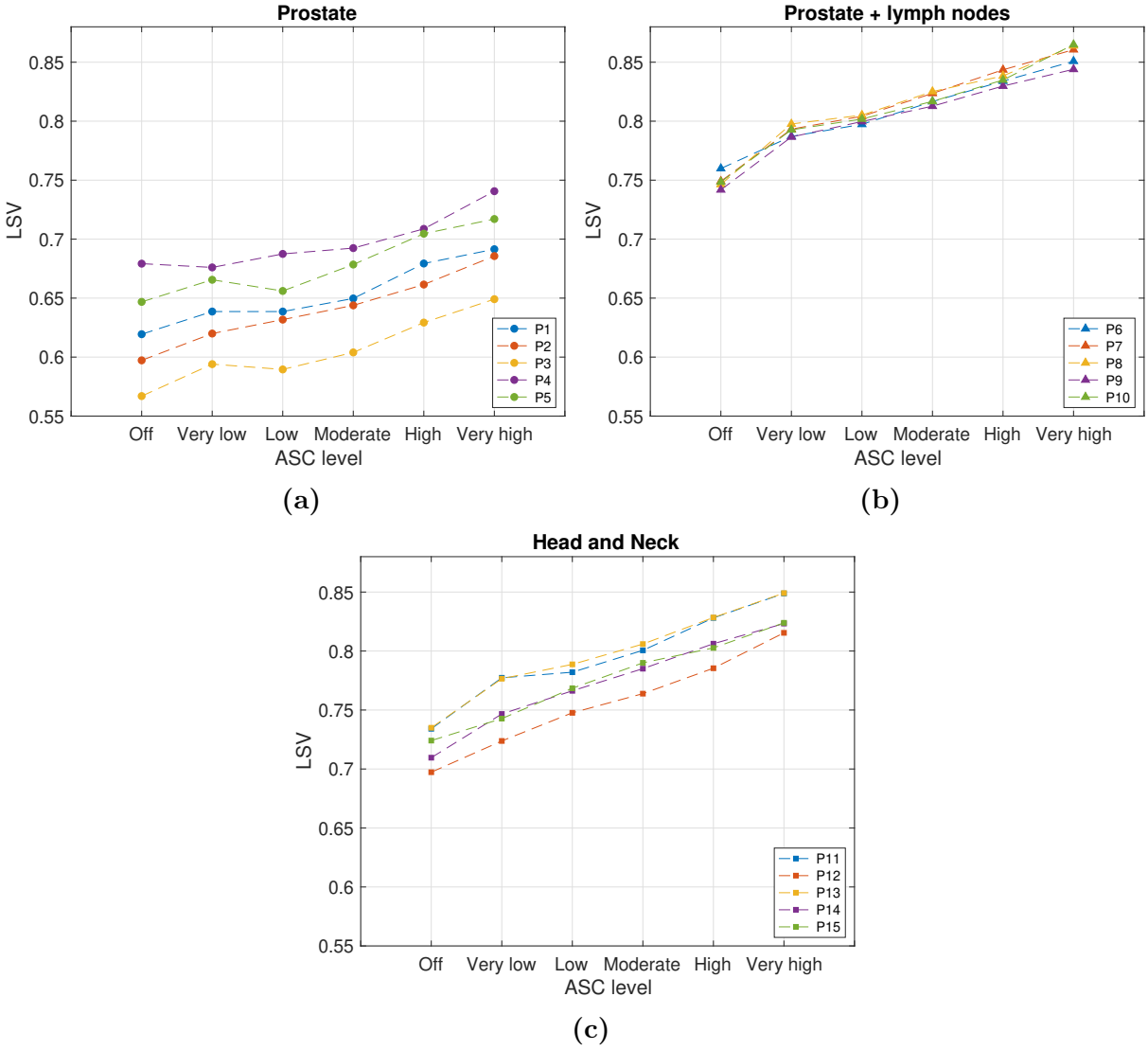

Figure 4.5: The mean LSV for each patient as a function of ASC level for the different cohorts; prostate **(a)**, prostate lgl **(b)** and H&N **(c)**.

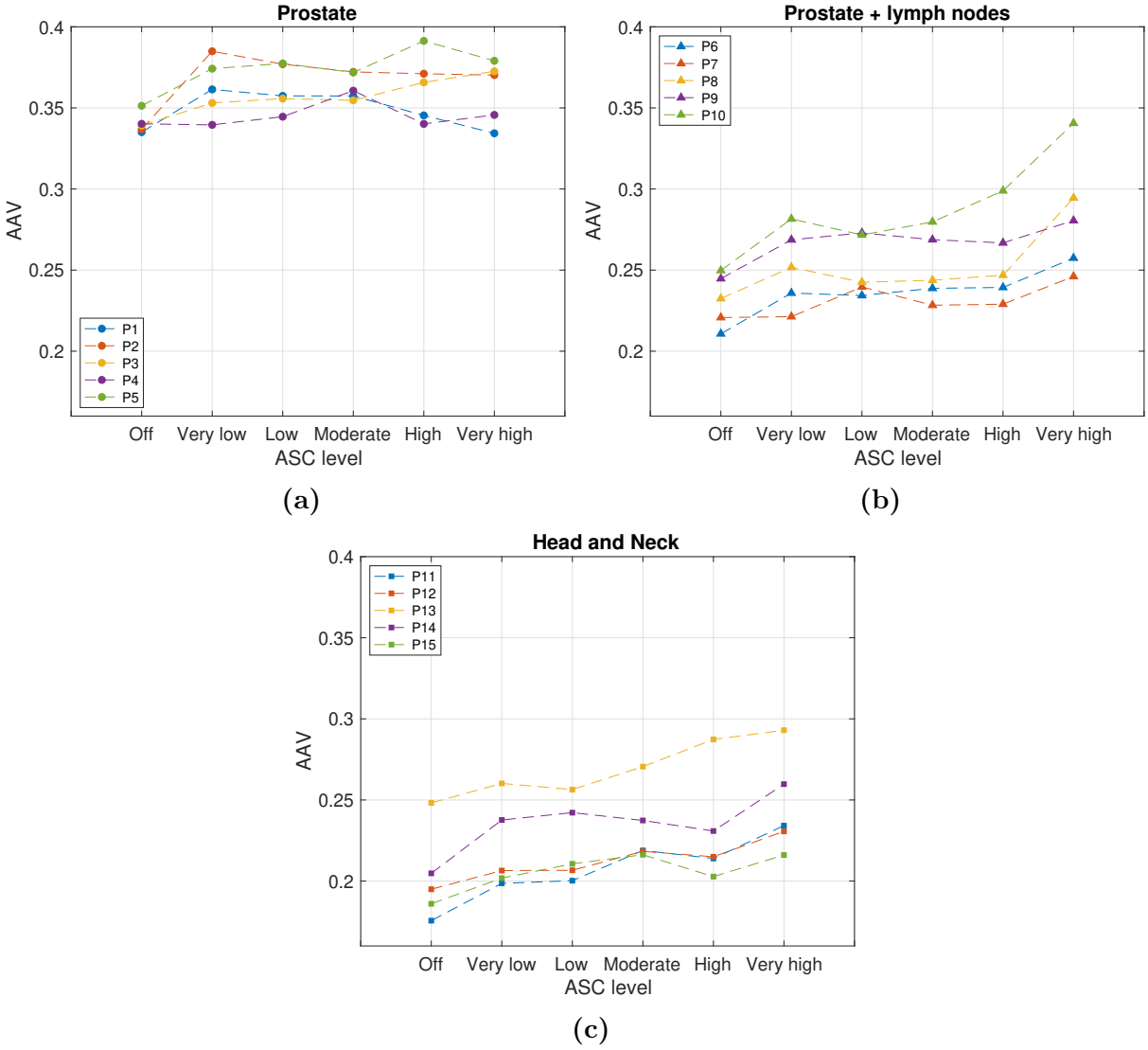

Figure 4.6: The mean AAV for each patient as a function of ASC level for the different cohorts; prostate **(a)**, prostate lgl **(b)** and H&N **(c)**.

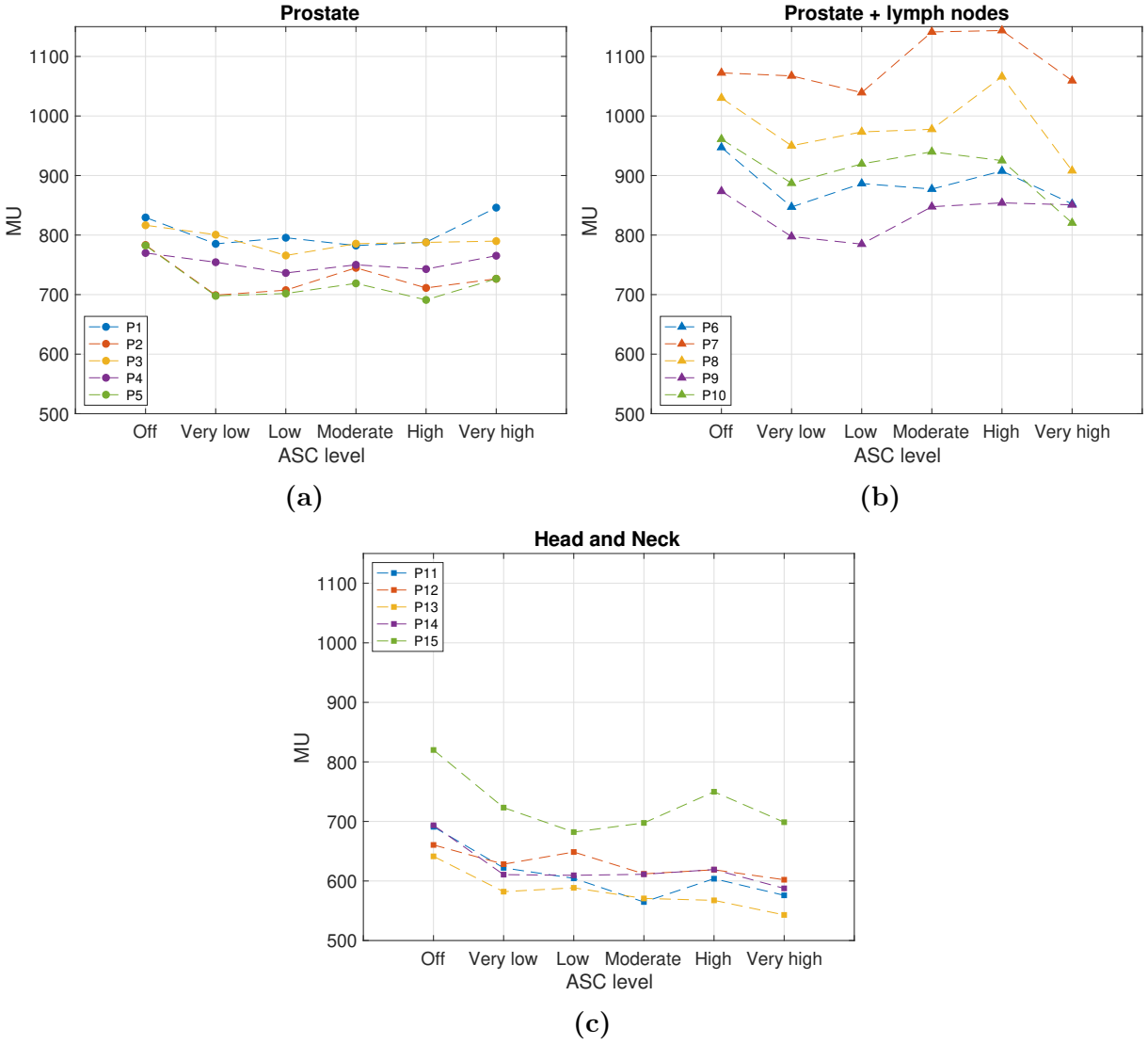

Figure 4.7: The total MU for each treatment plan as a function of ASC level for the different cohorts; prostate **(a)**, prostate lgl **(b)** and H&N **(c)**.

4.3 Measurements

The result from the measurements are presented in figure 4.8, were the left and right panels show the measured pass rate for the gamma criteria 3 % / 2 mm and 2% / 2 mm as a function of ASC level, respectively.

All treatment plans passed the clinical tolerances at SUS (90 % pass rate, 3 % / 2 mm). The lowest pass rate measured for the clinical criteria was 94.3 % for P10 (prostate lgl). No evident trend was observed between the pass rate and ASC level for any of the cohorts

(figure 4.8), this was also the case for the new base plans generated for P7 and P9. Large differences were observed between the patients. For example, P7 has a higher pass rate with ASC setting "Moderate" than "High". For the prostate lgl patients, the pass rate appears to deviate less between the cases for higher ASC levels.

The pass rates are presented as a function of the different complexity metrics in figures 4.9-4.11. Due to the prominent trend in figure 4.5, the pass rate was also plotted against the LSV. The AAV as a function of pass rate is shown in figure B.1 in Appendix B. Figures 4.9-4.11 shows no relationship.

For the prostate cases, a significant correlation was found for both the 3 % / 2 mm and 2 % / 2 mm pass rate. The 3 % / 2 mm pass rate correlated moderately with the EAM ($r_S = -0.736,\ p = 0.000$), MCS_v ($r_S = 0.517,\ p = 0.003$) and LSV ($r_S = 0.514,\ p = 0.004$. The 2 % / 2 mm pass rate correlated moderately with the EAM ($r_S = -0.619,\ p = 0.000$), a weak correlation was found for LSV ($r_S = 0.495,\ p = 0.005$) and MCS_v ($r_S = 0.369,\ p = 0.045$). These where the scores showing a stronger relationship with the ASC level (figure 4.4 and 4.5). No significant correlation was observed between any of the pass rates and complexity metrics for the prostate lgl and H&N cohorts. No obvious threshold value could be determined.

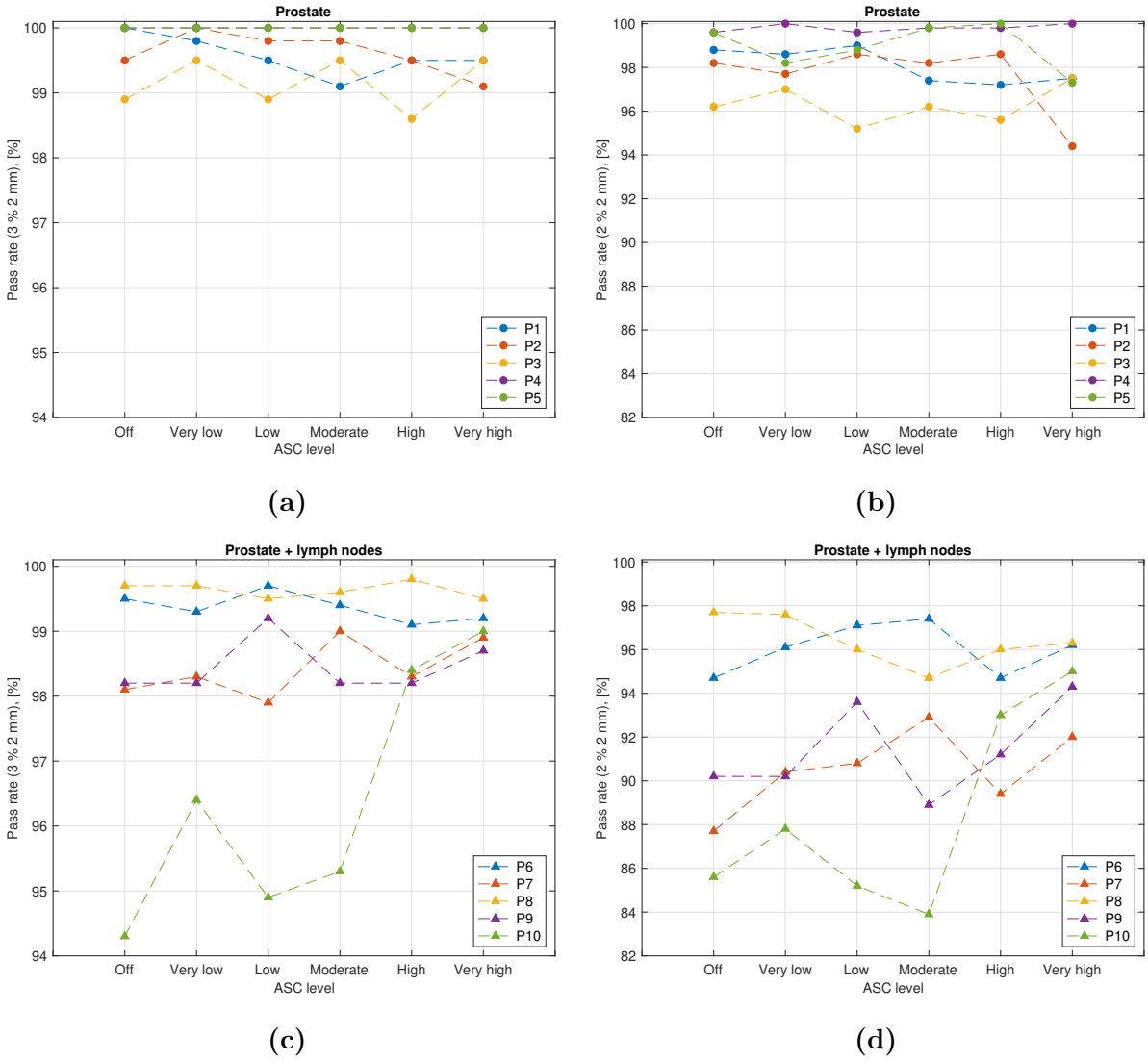

Figure 4.8: The pass rate as a function of ASC level for two different gamma criteria; 3 % 2 mm (left panel) 2 % 2 mm (right panel), for the different cohorts; prostate **(a)** and **(b)**, prostate lgl **(c)** and **(d)**, H&N **(e)** and **(f)**.

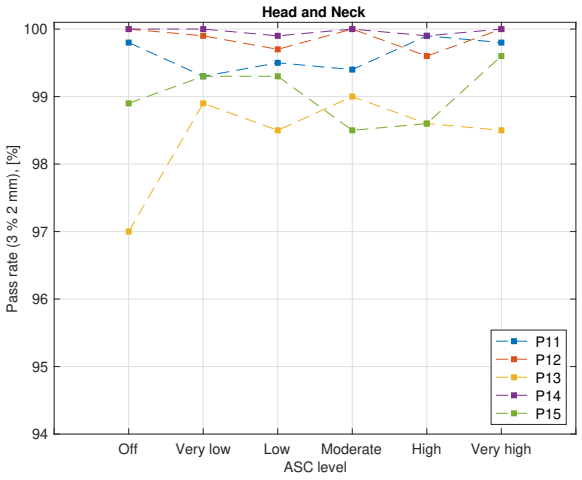

(e)

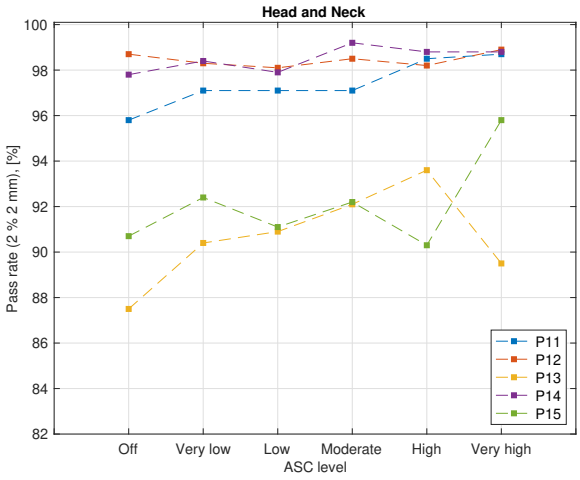

(f)

Figure 4.8: Continued.

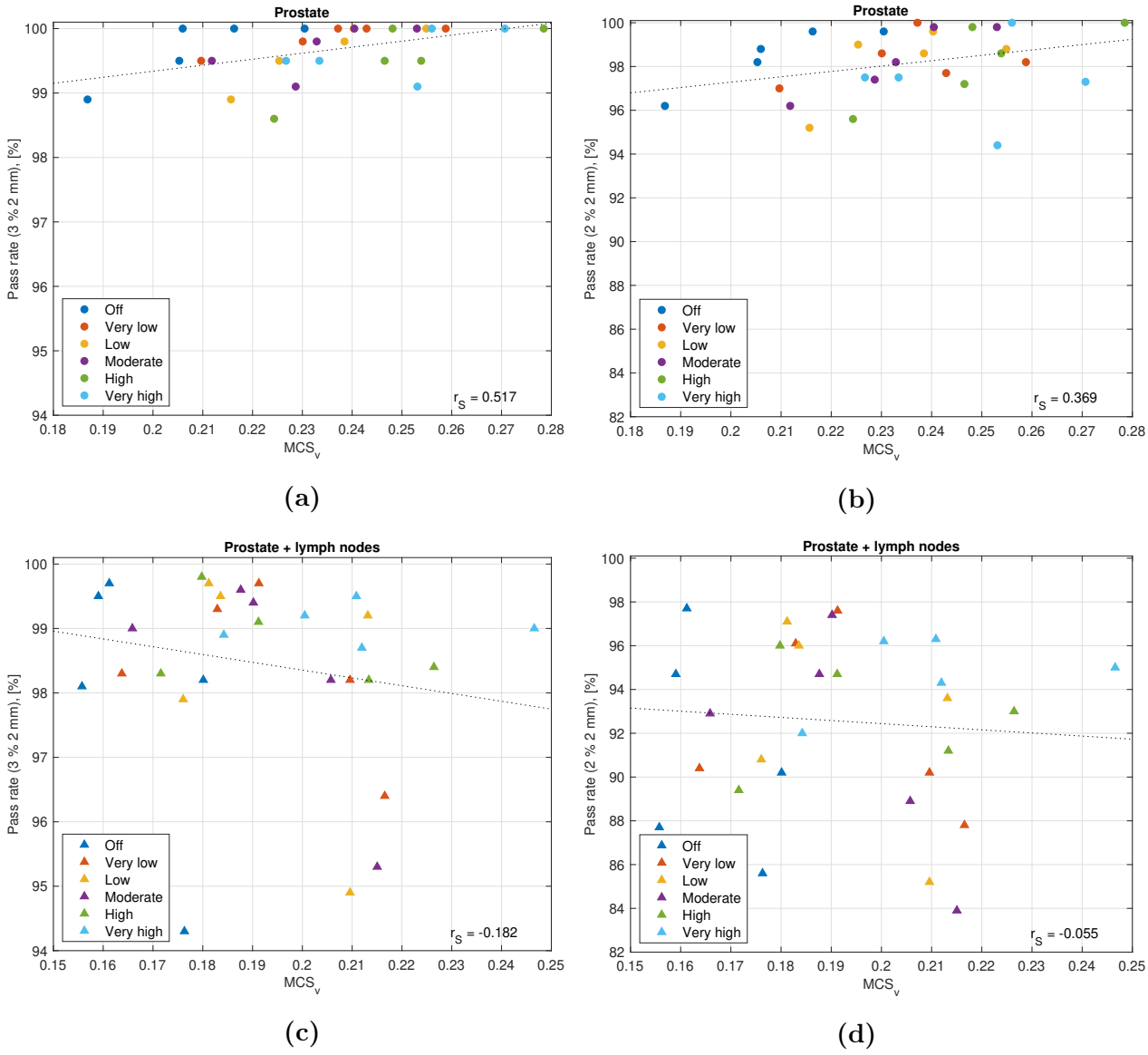

Figure 4.9: Gamma pass rate as a function of MCS_v for two different gamma criteria; 3 % 2 mm (left panel) 2 % 2 mm (right panel), for the different cohorts; prostate **(a)** and **(b)**, prostate lgl **(c)** and **(d)**, H&N **(e)** and **(f)**. High complexity is indicated by a low MCS_v value. The linear regression is represented by the dotted trend line, and Spearmans's r_S-values are denoted in the lower right corner.

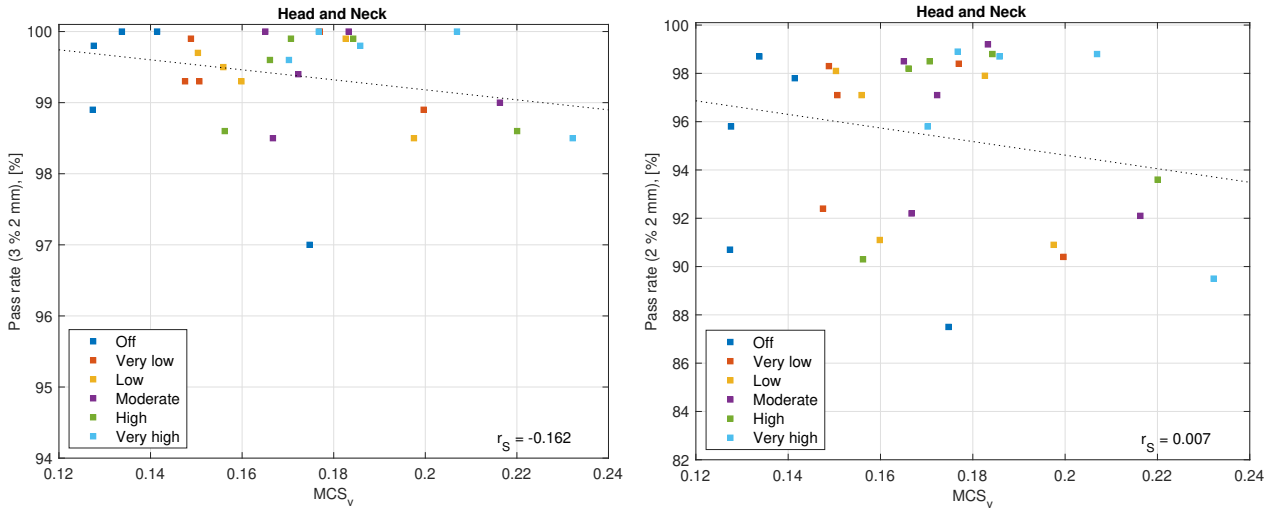

(e) (f)

Figure 4.9: Continued.

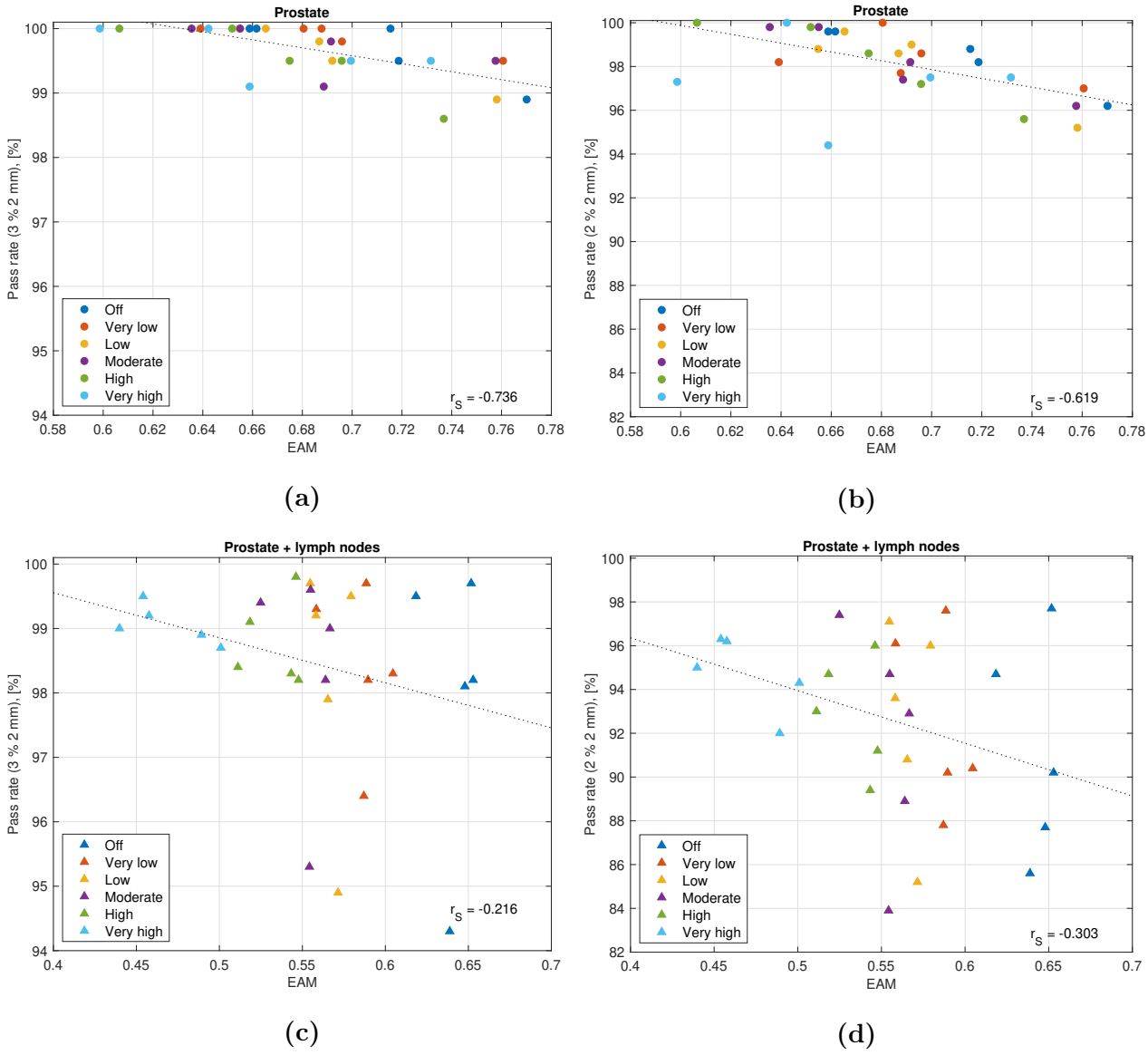

Figure 4.10: Gamma pass rate as a function of EAM for two different gamma criteria; 3 % 2 mm (left panel) 2 % 2 mm (right panel), for the different cohorts; prostate **(a)** and **(b)**, prostate lgl **(c)** and **(d)**, H&N **(e)** and **(f)**. High complexity is indicated by a high EAM value. The linear regression is represented by the dotted trend line, and Spearmans's r_S-values are denoted in the lower right corner.

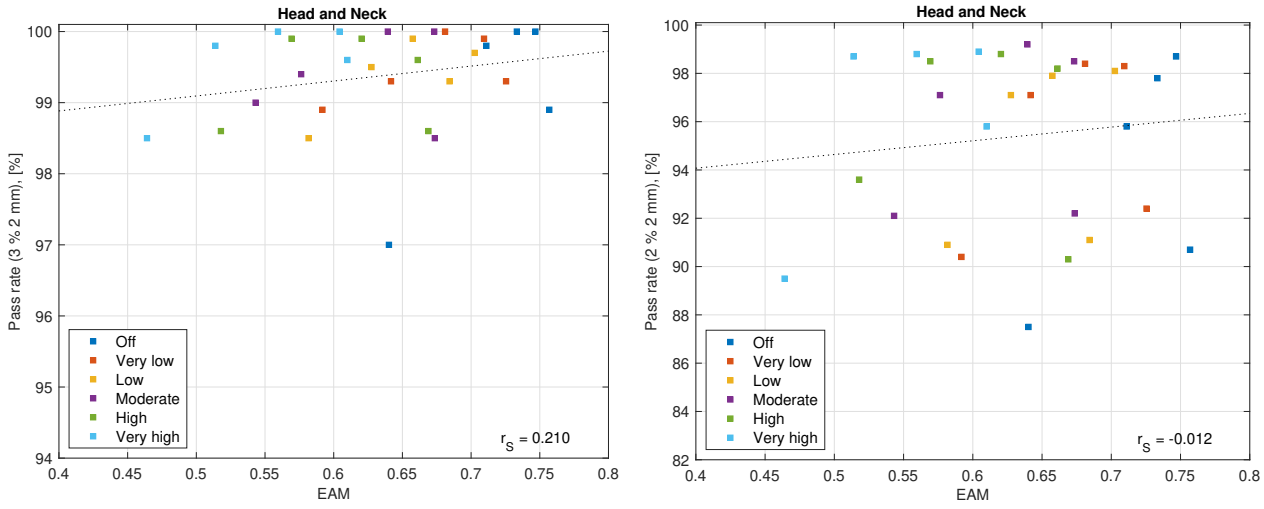

(e) (f)

Figure 4.10: Continued.

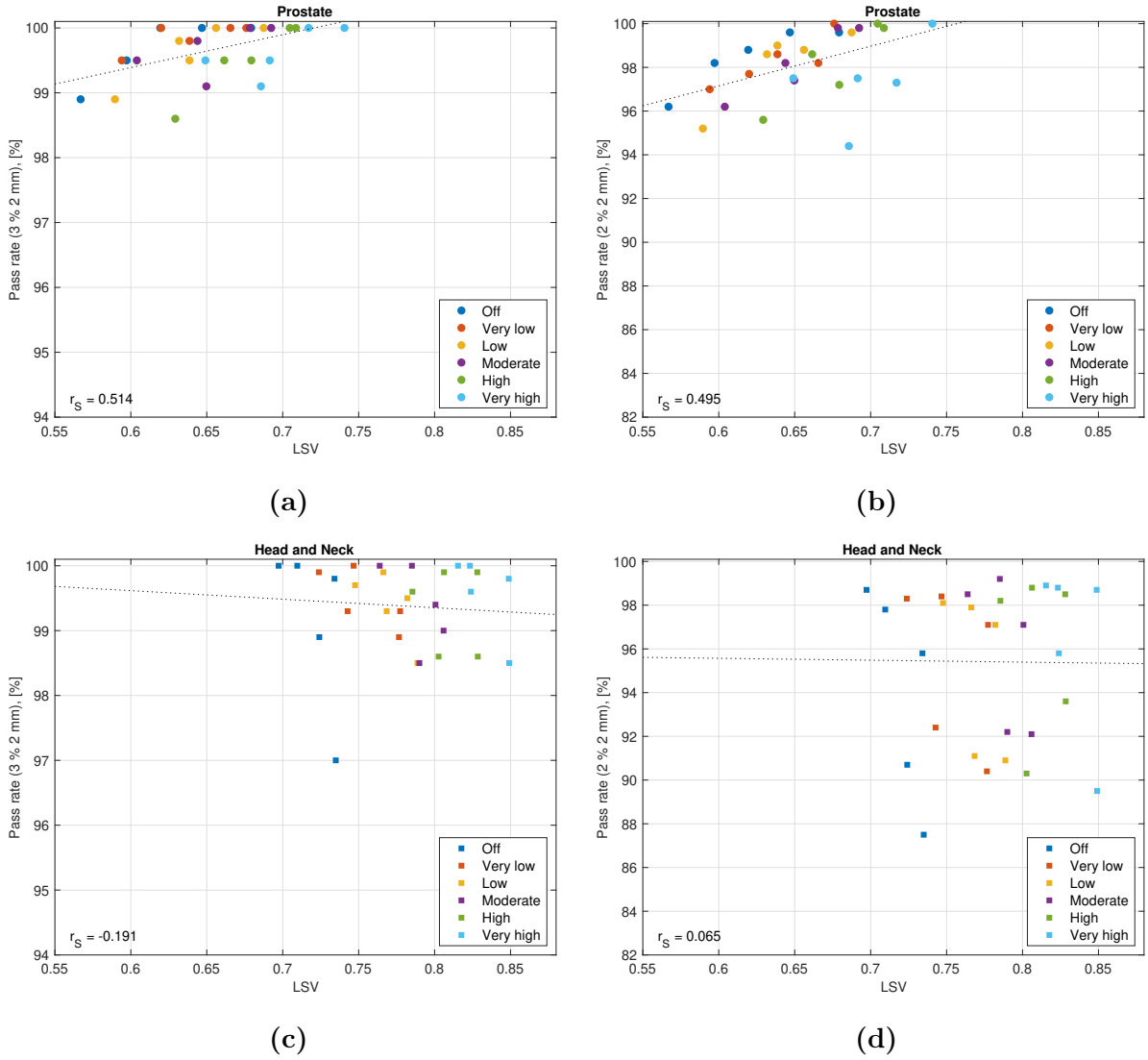

Figure 4.11: Gamma pass rate as a function of LSV for two different gamma criteria; 3 % 2 mm (left panel) 2 % 2 mm (right panel), for the different cohorts; prostate **(a)** and **(b)**, prostate lgl **(c)** and **(d)**, H&N **(e)** and **(f)**. The linear regression is represented by the dotted trend line, and Spearmans's r_S-values are denoted in the lower left corner.

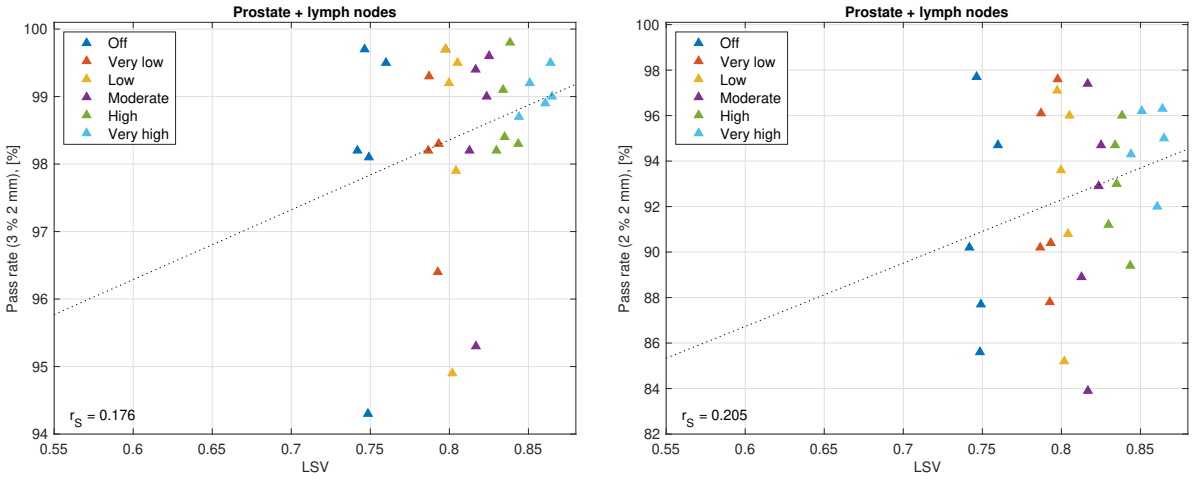

(e) **(f)**

Figure 4.11: Continued.

5. Discussion

5.1 Plan quality

The original plan for all patients were judged to be clinically acceptable. However, some of the plans did not meet all the objectives, as there is a trade off between PTV coverage and the OAR objectives. For these cases the priority of the dose constraints were followed. The dose distribution and plan complexity will differ for every re-optimization to some extent due to the inherent randomness in the optimization process. The penalization weight of the ASC is not known, meaning that it might not increase linearly with a higher ASC level.

The plan quality was in general not affected by a higher ASC setting, this is in agreement with previous studies on the ASC [27, 28, 29], they followed a similar approach by not changing the objectives during the optimization. Fog et al. [27] used both AAA and Acuros XB to calculate the dose distributions, while Binny et al. [28] used AAA and Scaggion et al. [29] used Acuros XB. Based on this, it seems that plan quality is not affected by the dose calculation algorithm to any great extent.

In this study, statistically sigficicant differences were found for some of the dosimetric parameters (table A.1), and the difference was most commonly found between the lower levels and the "Very high" setting. These differences were in general small and not considered to be clinically significant as other parameters will affect the outcome in a larger extent. Choosing a method where the objectives are changed individually during the optimization for every plan could have lead to bigger differences between a higher ASC level and the dosimetric parameters. Overall, these results indicates that "High" or a lower level might be optimal regarding plan quality.

5.2 Plan complexity

A higher ASC setting should reduce plan complexity. The most complex plan should be plans where the ASC is turned off and the least complex should be plans with ASC level "Very high". The general trend in figure 4.4 confirms this, but which plan that was the least complex varied between the patients and the two metrics. The ASC level "Very high" was the least complex for every patient except P1 for the EAM while for the MCS_v the ASC level "High" gave the lowest complexity for four patients (P1, P2, P5 and P9).

The higher EAM score for the prostate cohort compared to the prostate lgl cohort is probably due to that the score depends on the field size so it cannot be compared between different diagnosis.

The two scores depend on different parameters and therefore reflect different aspects of the VMAT segments. The main differences between them is that the MCS_v takes the variation in MU weight and relative area into consideration while the EAM is based on the relative size of the region around the MLC edges. However, indirectly the opening area is taken into account in the EAM. Plan complexity is often equated to the total amount of MUs i.e. reduced MU's for higher ASC settings, which is not reflected in figure 4.7. The relative area variation is not affected by a higher ASC level either, in figure 4.6, only a weak trend is observed. The EAM describes the differences between the ASC settings better than the MCS_v. Both the EAM and LSV (figure 4.4 and 4.5) indicates that ASC makes the MLC shape smoother. This could be more beneficial as the plan becomes less complex and it should not be as affected by internal movement compared to using smaller and irregular apertures.

Both Binny et al. [28] and Scaggion et al. [29] evaluated plan complexity using the MCS_v score. A decreased complexity for a higher ASC level was observed in both studies which agrees with the results presented here and the theory. They compared the ASC level with other complexity metrics as well, however, not with the EAM.

In general a higher setting than "Off" appears to generate a less complex plan with more even MLC shapes for all patients. However, it is not possible to determine whether "High" or "Very high" is the optimal level as it varies from patient to patient and depends on the metric of choice.

5.3 Plan verification and comparison

The gamma evaluation results in figure 4.8 shows that the pass rate does not generally increase with a higher ASC setting, but the variation in pass rate between patients appears to be reduced for higher ASC level. The highest pass rate seems to change between the levels, and no obvious threshold which resulted in a higher pass rate was observed. For the prostate only patients the pass rate differs, although never below 90 % for any ASC level using gamma criteria 3 % / 2 mm, which also was the case for prostate lgl and H&N. The pass rate seems to increase for a higher ASC setting for prostate lgl using the 3 % / 2 mm criteria. As for the 2 % / 2 mm, however, it decreases for some patients (P6 and P8) and increases for the others (P7, P9 and P10). The same variation was observed in the H&N cohort. This in patient variation makes it hard to settle on an optimal ASC level regarding plan verification. For some cases the "Very low" level has a higher pass rate than "Low" and "Moderate", and for some patients even better than "High" and "Very high" (P1 and P2 for 3 % / 2 mm for example).

Scaggion et al. [29] and Binny et al. [28] studied plan verification, however, using different measuring devices and gamma criterion. While Binny et al. [28] did not observe any im-

provements for the gamma pass rate for a higher ASC level, Scaggion et al. [29] did. The result presented in this thesis are in accordance with Binny et al. [28]. However, many different parameters could have affected the result, such as phantom device, phantom set up, dose calculation algorithms and so on, making it difficult to draw any direct conclusions.

The pass rate does not depend on the complexity of the plan. Figures 4.9-4.11 demonstrates the pass rate as a function of the different complexity metrics. The statistical tests concludes that a significance was only found for the prostate cohort for EAM, MCS_v and LSV. Although a significance was found, the strength of the correlation was only moderate or weak, especially for the 2 % / 2 mm pass rate. These plans were also the least complex plans but more similar to each other, therefore, a stronger correlation might be observed due to smaller patient-to-patient variation.

The fact that the ASC level does not seem to affect the pass rate could be due to the measurements not being sensitive enough. Another more sensitive method, for example film measurements, could have given results that are more in line with the theory. Measuring the plans several times at different occasions and calculating an average gamma pass rate value might be an alternative to a more sensitive plan verification as well as verifying the measurements with gafchromic film. It could also be that all treatment plans passed the clinical tolerance, indicating that the treatment plans are to some extent as good as they can get and a lower complexity does not affect the pass rate in any significant way. In a case where the initial treatment plan does not pass the gamma evaluation, incorporating a higher ASC level could make a larger impact, which have been observed in some clinical cases at SUS. A new treatment plan with a higher ASC level, where the same dose distribution was aimed for, passed the clinical tolerance. As mentioned earlier, a method where the objectives are changed for every plan could have generated a different result.

6. Conclusion

In general, the plan complexity decreased without compromising plan quality for higher ASC levels. However, a better consistency between the planned and measured dose was not found. An ASC level between "Very low" and "High" is optimal, due to the in patient variation for the plan verification and that the plan quality is not affected and the plan complexity is reduced for these levels.

7. Future work

There are only a few studies published about the ASC, and more extensive investigations needs to be performed. Since the size of the cohorts were small in this study, a natural next step would be to include more patients. Further and more extensive examinations of the measurement results, where every point is investigated, would also be of value. Studying other treatment sites is also of interest. Another way to pinpoint the influence of the ASC level on measurement results could be to re-optimize clinical treatment plans that fail the gamma analysis with a higher ASC setting. Smaller and irregular apertures will to a larger extent be more affected by external and internal movement. This could be investigated by introducing motion into the measurements. Hopefully, further studies can find a more apparent relationship, if there is one, between plan complexity, ASC level and pass rate to find the threshold value which determines whether a QC measurements is needed or not.

Bibliography

[1] Cancerfonden. Cancerfondsrapporten 2018 [Internet]. Stockholm; Cancerfonden; 2018. [2020-02-11]. Available from: https://static-files.cancerfonden.se/Cancerfondsrapporten2018_webb_(2)_1521607903.pdf.

[2] Cancerfonden. Statistik om cancer [Internet]. Stockholm; Cancerfonden; 2018. [2020-02-11]. Available from: https://www.cancerfonden.se/om-cancer/statistik.

[3] Söderlund Leifler K, Landberg T. Strålbehandling [Internet]. Nationalencyklopedin; c 2020. [2020-03-18]. Available from: http://www.ne.se.ludwig.lub.lu.se/uppslagsverk/encyklopedi/lång/strålbehandling.

[4] Podgorsak EB, SpringerLink. Radiation Physics for Medical Physicists [Internet]. Graduate Texts in Physics. Springer International Publishing; 2016. [2020-03-18]. Available from: https://link-springer-com.ludwig.lub.lu.se/book/10.1007%2F978-3-319-25382-4.

[5] Brahme A. Optimization of stationary and moving beam radiation therapy techniques. Radiotherapy and oncology : journal of the European Society for Therapeutic Radiology and Oncology. 1988;12(2):129 – 140. Available from: https://doi.org/10.1016/0167-8140(88)90167-3.

[6] Yu CX. Intensity-modulated arc therapy with dynamic multileaf collimation: an alternative to tomotherapy. Physics in Medicine and Biology. 1995;40(9):1435 – 1449. Available from: https://iopscience-iop-org.ludwig.lub.lu.se/article/10.1088/0031-9155/40/9/004/pdf.

[7] Otto K. Volumetric modulated arc therapy: IMRT in a single gantry arc. Medical Physics. 2008;35(1):310 – 317. Available from: https://aapm-onlinelibrary-wiley-com.ludwig.lub.lu.se/doi/full/10.1118/1.2818738.

[8] Bortfeld T. IMRT: a review and preview. Physics in Medicine and Biology. 2006;51(13):R363–R379. Available from: https://doi.org/10.1088%2F0031-9155%2F51%2F13%2Fr21.

[9] Teoh M, Clark CH, Wood K, Whitaker S, Nisbet A. Volumetric modulated arc therapy: a review of current literature and clinical use in practice. The British Journal Of Radiology. 2011;84(1007):967 – 996. Available from: https://doi.org/10.1259/bjr/22373346.

[10] Yu CX, Tang G. Intensity-modulated arc therapy: principles, technologies and clinical implementation. Physics in Medicine and Biology. 2011 feb;56(5):R31–R54. Available from: https://doi.org/10.1088%2F0031-9155%2F56%2F5%2Fr01.

[11] Das IJ, Ding GX, Ahnesjö A. Small fields: nonequilibrium radiation dosimetry. Medical physics (Lancaster). 2008;(1):206. Available from: https://aapm-onlinelibrary-wiley-com.ludwig.lub.lu.se/doi/epdf/10.1118/1.2815356.

[12] Varian Medical Systems I. Eclipse Photon and Electron Algorithms Reference Guide. Palo Alto; Varian Medical Systems, Inc; 2017. [2020-03-20].

[13] Malmquist J, Cederblom S. Datortomografi [Internet]. Nationalencyklopedin; c 2020. [2020-04-21]. Available from: http://www.ne.se.ludwig.lub.lu.se/uppslagsverk/encyklopedi/lång/datortomografi.

[14] ICRU. Report 83. Journal of the International Commission on Radiation Units and Measurements: Oxford University Press. 2016 06;10(1):NP–NP. Available from: https://doi.org/10.1093/jicru/10.1.Report83.

[15] Knöös T, Wieslander E, Cozzi L, Brink C, Fogliata A, Albers D, et al. Comparison of dose calculation algorithms for treatment planning in external photon beam therapy for clinical situations. Physics in Medicine and Biology. 2006;51(22):5785 – 5807. Available from: https://pubmed.ncbi.nlm.nih.gov/17068365/?from_term=Brink+C&from_cauthor_id=17068365&from_pos=1.

[16] Ojala JJ, Kapanen MK, Hyödynmaa SJ, Wigren TK, Pitkänen MA. Performance of dose calculation algorithms from three generations in lung SBRT: comparison with full Monte Carlo-based dose distributions. Journal of applied clinical medical physics. 2014;15(2):4662. Available from: https://aapm-onlinelibrary-wiley-com.ludwig.lub.lu.se/doi/full/10.1120/jacmp.v15i2.4662.

[17] McNiven AL, Sharpe MB, Purdie TG. A new metric for assessing IMRT modulation complexity and plan deliverability. Medical Physics. 2010;37(2):505 – 515. Available from: https://aapm-onlinelibrary-wiley-com.ludwig.lub.lu.se/doi/10.1118/1.3276775.

[18] Götstedt J, Karlsson Hauer A, Bäck A. Development and evaluation of aperture-based complexity metrics using film and EPID measurements of static MLC openings. Medical Physics. 2015;42(7):3911–3921. Available from: https://aapm.onlinelibrary.wiley.com/doi/abs/10.1118/1.4921733.

[19] Chiavassa S, Bessieres I, Edouard M, Mathot M, Moignier A. Complexity metrics for IMRT and VMAT plans: a review of current literature and applications. The British Journal Of Radiology. 2019;92(1102):20190270. Available from: https://www.birpublications.org/doi/pdf/10.1259/bjr.20190270.

[20] Wolff D, Stieler F, Welzel G, Lorenz F, Abo-Madyan Y, Mai S, et al. Volumetric modulated arc therapy (VMAT) vs. serial tomotherapy, step-and-shoot IMRT and 3D-conformal RT for treatment of prostate cancer. Radiotherapy and Oncology. 2009;93(2):226 – 233. Available from: http://www.sciencedirect.com/science/article/pii/S0167814009004472.

[21] Matuszak MM, Yan D, Grills I, Martinez A. Clinical Applications of Volumetric Modulated Arc Therapy. International Journal of Radiation Oncology*Biology*Physics. 2010;77(2):608 – 616. Available from: http://www.sciencedirect.com/science/article/pii/S0360301609029836.

[22] Oliver M, Gagne I, Bush K, Zavgorodni S, Ansbacher W, Beckham W. Clinical significance of multi-leaf collimator positional errors for volumetric modulated arc therapy. Radiotherapy and Oncology. 2010;97(3):554 – 560. Available from: http://www.sciencedirect.com/science/article/pii/S0167814010004639.

[23] Masi L, Doro R, Favuzza V, Cipressi S, Livi L. Impact of plan parameters on the dosimetric accuracy of volumetric modulated arc therapy. Medical Physics. 2013;40(7). Available from: https://aapm-onlinelibrary-wiley-com.ludwig.lub.lu.se/doi/10.1118/1.4810969.

[24] ScandiDos. Delta^4 Phantom+ - The Wireless Phantom. Uppsala; ScandiDos AB; c 2020. [2020-04-02]. Available from: https://delta4family.com/upload/documents/brochures/Delta4%20Phantom%20plus.pdf.

[25] Paddick I. A simple scoring ratio to index the conformity of radiosurgical treatment plans. Technical note. Journal Of Neurosurgery. 2000;93 Suppl 3:219 – 222. Available from: https://pdfs.semanticscholar.org/89e3/7c306d5f14c39567e924d5b8f53a2c09c979.pdf.

[26] Low DA, Harms WB, Mutic S, Purdy JA. A technique for the quantitative evaluation of dose distributions. Medical Physics. 1998;25(5):656 – 661. Available from: https://aapm-onlinelibrary-wiley-com.ludwig.lub.lu.se/doi/10.1118/1.598248.

[27] Fog L, Offer K, Hardcastle N. EP-1814 On the aperture shape controller and the air cavity correction for lung plans using AcurosXB and AAA. Radiotherapy and Oncology. 2019;133:S983. ESTRO 38, 26-30 April 2019, Milan, Italy. Available from: http://www.sciencedirect.com/science/article/pii/S0167814019322340.

[28] Binny D, Spalding M, Crowe SB, Jolly D, Kairn T, Trapp JV, et al. Investigating the use of aperture shape controller in VMAT treatment deliveries. Medical Dosimetry. 2020;45(3):284 – 292. Available from: http://www.sciencedirect.com/science/article/pii/S095839472030025X.

[29] Scaggion A, Fusella M, Agnello G, Bettinelli A, Pivato N, Roggio A, et al. Limiting treatment plan complexity by applying a novel commercial tool. Journal of

Applied Clinical Medical Physics. 2020;21(8):27–34. Available from: `https://aapm.onlinelibrary.wiley.com/doi/abs/10.1002/acm2.12908`.

A. Appendix A

A.1 Plan quality

The results of the Friedmans tests and the post hoc Wilcoxon tests for the dosimetric parameters showing a statistically significant difference are summarized in table A.1.

Table A.1: The result of the Friedman's test for the dosimetric parameters showing a statistical significance, and the Wilcoxon's signed rank test result for these parameters where a significance between the ASC levels were observed.

Cohort	Parameter	Friedman's test p-value	Level compared	Wilcoxon's test p-value
Prostate	$D_{\text{min,CTV}}$	0.048	Off - High[a]	0.043
			Off - Very high[a]	0.043
			Very low - Very high[a]	0.043
			Moderate - Very high[a]	0.043
Prostate + nodes	$D_{\text{min,CTV}}$	0.020	Off - Very low[a]	0.043
			Off - High[a]	0.043
			Low - Moderate[b]	0.043
			Moderate - High[a]	0.043
			Moderate - Very high[a]	0.043
	$D_{20\%,\text{Rectum}}$	0.046	Off - Very high[a]	0.043
			Very low - Very high[a]	0.043
			Low - Very high[a]	0.043
			Moderate - Very high[a]	0.043
			High - Very high[a]	0.043
	$D_{15\%,\text{Rectum}}$	0.032	Off - Very high[a]	0.043
			Very low - Very high[a]	0.043
			Low - Very high[a]	0.043
			High - Very high[a]	0.043
	$D_{99\%,\text{PTV}}$	0.035	Off - Low[b]	0.043
			Off - Very high[b]	0.043
			Very low - Very high[b]	0.043
			Low - Very high[b]	0.043
			Moderate - Very high[b]	0.043
			High - Very high[b]	0.043
	$D_{\text{max,FH}_R}$	0.040	Off - Very high[b]	0.043
			Very low - Very high[b]	0.043
			Low - Very high[b]	0.043
			Moderate - Very high[b]	0.043
	$V_{30\text{Gy,BB}}$	0.008	Off - Very high[b]	0.043
			Very low - Very high[b]	0.043
			Low - Moderate[a]	0.043
			Low - Very high[b]	0.043
			Moderate - High[b]	0.043
			Moderate - Very high[b]	0.043
	$V_{50\text{Gy,BB}}$	0.022	-	-

BB; Bowelbag; FH: Femoral head; L:Left.
[a] signifies that the higher ASC level showed a better result than the lower. [b] signifies that the higher ASC level showed a worse result than the lower. For CTV/PTV, [a] and [b] means better and worse coverage for a higher level, respectively. For OARs, [a] and [b] stands for a lower and higher dose for a higher level, respectively. For CI and HI, [a] and [b] denotes better and worse conformity and homogeneity for a higher level, respectively.

Table A.1: Continued.

Cohort	Parameter	Friedman's test p-value	Level compared	Wilcoxon's test p-value
Prostate + nodes	CI	0.030	Off - Very high[b]	0.042
			Very low - Very high[b]	0.043
			Low - Very high[b]	0.043
			Moderate - Very high[b]	0.043
			High - Very high[b]	0.042
	HI	0.023	Very low - Very high[b]	0.043
			Low - Very high[b]	0.043
			Moderate - Very high[b]	0.043
			High - Very high[b]	0.042
Head & Neck	CI	0.025	Off - High[a]	0.042
			Off - Very high[a]	0.043
			Very low - Very high[a]	0.043
			Low - Very high[a]	0.039
	HI	0.047	Very low - Very high [b]	0.042
			High - Very high [b]	0.042

B. Appendix B

B.1 Measurements

The pass rate as a function of AAV is shown in figure B.1 together with the Spearmans r_S-value. No statistically significant correlation was found for any of the pass rates or cohorts.

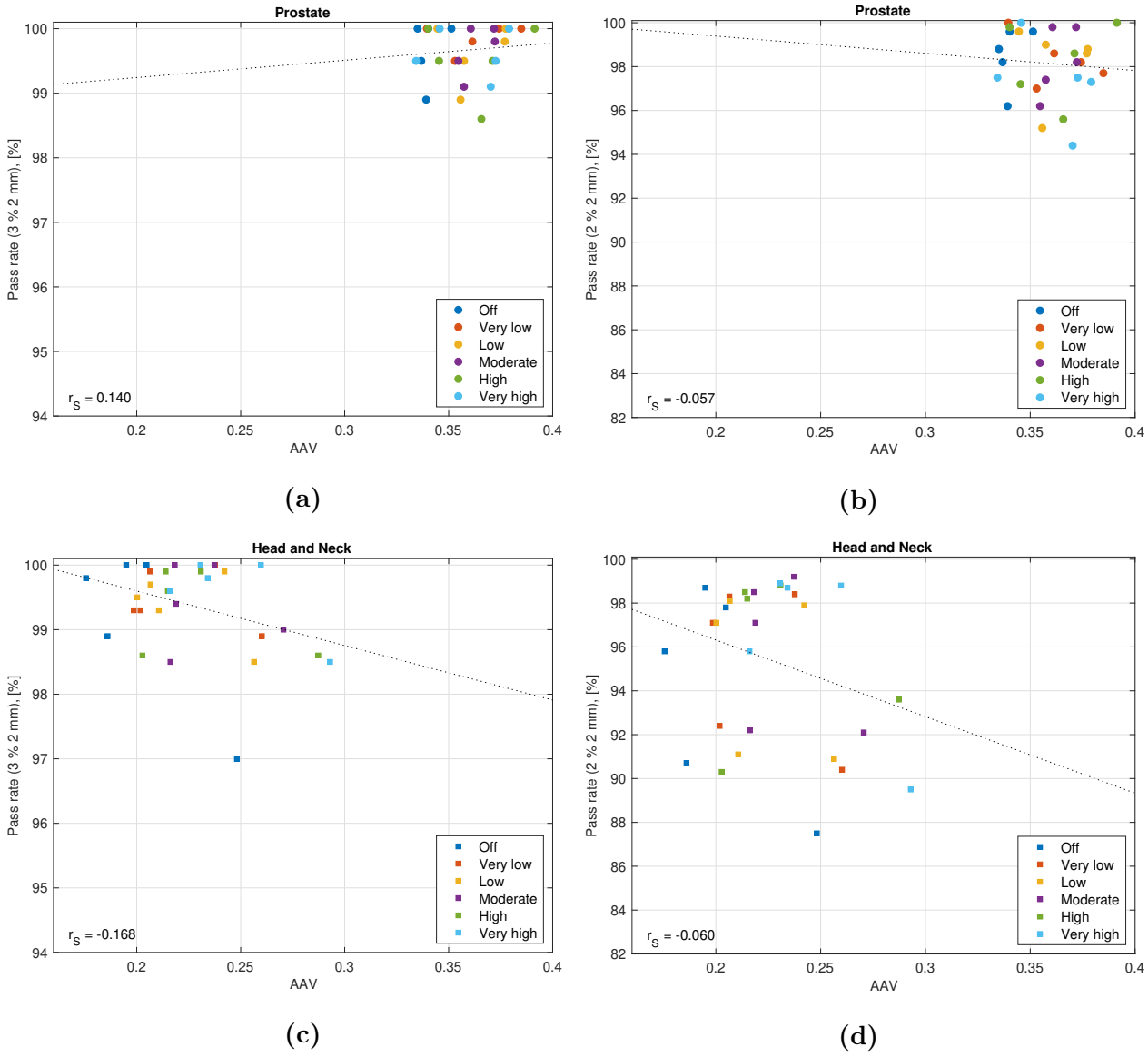

Figure B.1: Gamma pass rate as a function of AAV for two different gamma criteria; 3 % 2 mm (left panel) 2 % 2 mm (right panel), for the different cohorts; prostate **(a)** and **(b)**, prostate lgl **(c)** and **(d)**, H&N **(e)** and **(f)**. The linear regression is represented by the dotted line, and Spearmans's r_S-values are denoted in the lower left corner.

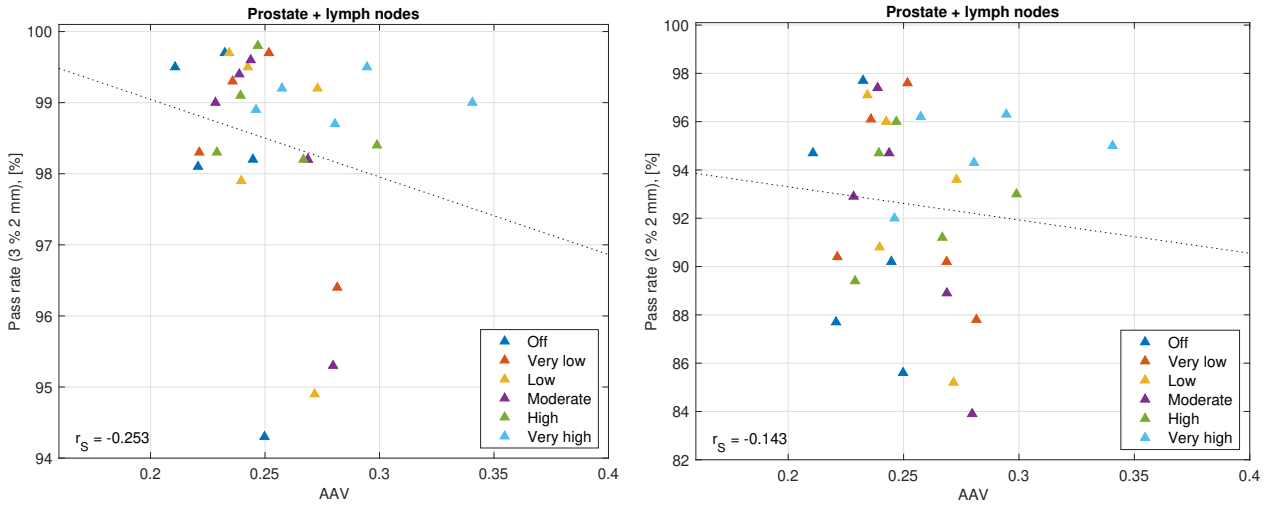

(e) (f)

Figure B.1: Continued.